



## Review

Gold nanorod-based localized surface plasmon resonance biosensors:  
A reviewJie Cao <sup>a,\*</sup>, Tong Sun <sup>a</sup>, Kenneth T.V. Grattan <sup>a,b</sup><sup>a</sup> School of Engineering and Mathematical Sciences, City University London, London EC1V 0HB, UK<sup>b</sup> City Graduate School, City University London, London EC1V 0HB, UK

## ARTICLE INFO

## Article history:

Received 7 November 2013

Received in revised form 7 January 2014

Accepted 16 January 2014

Available online 25 January 2014

## Keywords:

Localized surface plasmon resonance

LSPR

Gold nanorod

Biosensors

Nanoparticles

Optical fiber sensor

## ABSTRACT

Noble metal nanoparticle-based localized surface plasmon resonance (LSPR) is an advanced and powerful label-free biosensing technique which is well-known for its high sensitivity to the surrounding refractive index change in the local environment caused by the biomolecular interactions around the sensing area. The characteristics of the LSPR effect in such sensors are highly dependent on the size, shape and nature of the material properties of the metallic nanoparticles considered. Among the various types of metallic nanoparticles used in studies employing the LSPR technique, the use of gold nanorods (GNRs) has attracted particular attention for the development of sensitive LSPR biosensors, this arising from the unique and intriguing optical properties of the material. This paper provides a detailed review of the key underpinning science for such systems and of recent progress in the development of a number of LSPR-based biosensors which use GNR as the active element, including an overview of the sensing principle, the synthesis of GNRs, the fabrication of a number of biosensors, techniques for surface modification of GNRs and finally their performance in several biosensing applications. The review ends with a consideration of key advances in GNR-based LSPR sensing and prospects for future research and advances for the development of the GNR-based LSPR biosensors.

© 2014 Elsevier B.V. All rights reserved.

## Contents

1. Introduction .....	333
2. Principles of LSPR .....	334
3. Synthesis of GNRs .....	336
3.1. Seed-mediated growth method .....	336
3.2. Electrochemical method .....	337
3.3. Template method .....	337
3.4. Electron beam lithography method .....	338
3.5. Other methods .....	338
4. Surface modification of the CTAB-capped GNRs .....	340
4.1. Surface covering .....	340
4.2. Ligand exchange .....	341
5. GNR-based LSPR biosensors .....	343
5.1. Chip-based LSPR sensor .....	343
5.2. Optical fiber-based LSPR sensors .....	344
5.3. Solution-phase-based LSPR sensor .....	345
6. Advances in LSPR biosensing .....	347
6.1. Multiplexed biosensing .....	347
6.2. Single-nanoparticle based LSPR biosensing .....	348

\* Corresponding author at: School of Engineering and Mathematical Sciences, City University London, Room CG43, Tait Building, London EC1V 0HB, UK.  
Tel.: +44 020 7040 3641.

E-mail address: [jie.cao.1@city.ac.uk](mailto:jie.cao.1@city.ac.uk) (J. Cao).

7. Conclusion and future outlook.....	348
Acknowledgements.....	349
References.....	349
Biographies.....	351

---

## 1. Introduction

Biosensors have been continuing to play an important role in many scientific fields including clinical diagnostics, medical developments, illicit drug detection, food quality and safety, and environmental monitoring [1]. Their importance is seen in that each is a multi-billion dollar areas of activity and vitally important for the well-being of people the world over. A biosensor can be defined as an analytical device which comprises two basic components: a recognition unit used to capture the specific target, and a transducer that can convert the subtle biomolecular interactions into the quantifiable signal [2], which is usually electrical in nature. However, recent developments have seen an enormous growth in biosensors based on optical transducer principles, such as those using techniques such as fluorescence [3–5], surface plasmon resonance (SPR) [6–8] and chemiluminescence [9,10], which have been developed for a wide range of applications. Among the various optical biosensors reported in the literature, SPR-based biosensors show a number of significant advantages over conventional sensors, including ultra-high refractive index sensitivity, fast sensor response, real-time detection, and a label-free technique. In addition, the advanced nature of SPR imaging (SPRI) technology not only retains these advantages of classical SPR sensing, but also allows the detection of target molecules on a biosensor chip to be visualized in real-time by using a CCD camera [11]. Thus SPR biosensors have been studied extensively and developed and commercialized in the past three decades in particular. SPR is an optical phenomenon where the surface conductive electrons of bulk metal oscillate collectively at their resonant frequency, and the electron oscillations propagate along the metal-dielectric interface and decay exponentially into both media [12]. However, in order to fabricate a SPR sensor chip, sophisticated instrumentation such as a sputter coater or vacuum evaporator is normally required to coat the noble metal film on the surface of an optical substrate, such as a prism and an optical fiber, to excite SPR. In addition, most commercial SPR instruments, such as the well-known Biacore™ series, are normally expensive and bulky, which limits the extent of their applications.

In recent years, biosensors based on localized surface plasmon resonance (LSPR), which is also a SPR phenomenon but exists in metallic nanoparticles (MNPs) rather than bulk metal, has attracted more and more attention. The physical properties of the noble metals change enormously from what is usually familiar when the size of these metal particles is on the nanoscale level and smaller than the wavelength of the light used to illuminate them [13,14]. A particularly striking example is that the color of gold in the nanoworld is no longer the familiar ‘gold color’ but it can be as colorful as a rainbow, as shown in Fig. 1. Here gold nanorods (GNRs), with various aspect ratios and suspended in aqueous solutions, display a range of different colors. The SPR phenomenon also changed from SPR to LSPR when the bulk metal film was replaced by MNPs to excite SPR. Here the properties of LSPR are highly dependent on the material used and the size and shape of the metallic nanoparticles involved [14]. By manipulating these parameters, the LSPR wavelength can conveniently be tuned throughout the visible, near-infrared, and into the infrared region, allowing the LSPR sensor to be constructed for particular applications where a specific wavelength is desired. Compared to SPR sensors, LSPR sensors are of more flexible design and lower cost in terms of sensor fabrication, arising from the fact that LSPR can be excited when the light directly

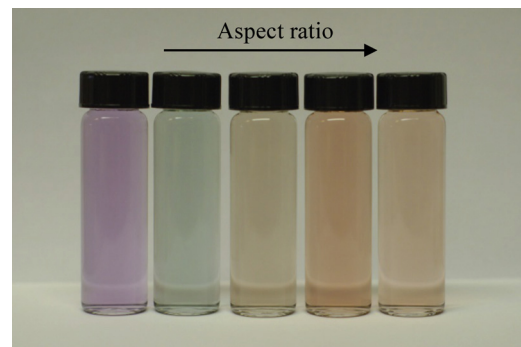


**Fig. 1.** Photograph of GNRs solutions with different aspect ratios showing the different colors of the solutions that result.

interacts with the MNPs and free from the need for prisms or other optical components. For instance, LSPR sensors can either be fabricated by immobilizing MNPs on a substrate, such as glass slide [15] or an optical fiber [16], or by simply suspending MNPs in solution to form a solution-phase based LSPR sensor [17]. In addition, as LSPR is highly localized at each individual MNPs, LSPR sensors can even be fabricated based on single nanoparticle [18]. Moreover, some LSPR biosensors have demonstrated superior sensitivity in comparison with the traditional bulk metal film based SPR biosensors [19], making them particularly attractive to use. These advantages of LSPR biosensors have prompted significant effort to be devoted to the development of sensitive LSPR biosensors and numerous promising LSPR biosensor designs continue to be reported in the literature, as this review emphasizes.

The advances seen in the fabrication of MNPs have led to considerable progress in the development of a range of LSPR biosensors in the past decade. Early research on the development of LSPR biosensor had mainly been focused on the use of spherical gold nanoparticles, due to their ease of synthesis. However recent developments have allowed a number of LSPR sensors, based on noble MNPs and of various shapes, to be developed and these have shown both higher sensitivities and other important advantages, in comparison to using gold nanosphere-based (GNS) LSPR sensors. Among these MNPs recently reported, GNRs have demonstrated unique optical properties, such as higher refractive index sensitivity and a tuneable longitudinal plasmon band, achieved by adjusting their aspect ratio [20,21] and thus allowing them to show excellent characteristics as LSPR biosensors. In addition to LSPR sensing, GNRs have also been applied in many other fields such as SERS sensing [22], chemical imaging [23] and in cancer therapy [24].

Despite the fact that several excellent and well cited reviews on the general LSPR biosensors have been reported previously, these past reviews have not focused particularly on LSPR biosensors based on GNRs, to the best of our knowledge. This aspect is addressed directly in this paper which is designed to supplement the body of knowledge in this area by reviewing both key fundamental aspects and recent progress on the development of GNR-based LSPR biosensors. The paper thus deals with an overview of the underpinning sensing principles, the synthesis of GNRs, the surface modification of GNRs, the fabrication of a number of different biosensors and a range of biosensing applications, followed by a discussion of advances in GNR-based LSPR sensing. The paper

ends with a view of future potential directions in research in this field.

## 2. Principles of LSPR

MNPs have particular optical properties which are significantly different from those observed in the bulk metal. When incident light interacts with MNPs, the electromagnetic field of the light induces a collective coherent oscillation of the surface conduction electrons of the MNPs in resonance with the frequency of light, in a phenomenon known as LSPR [14,25]. The electric field of the light interacts with the free electrons in the nanoparticles, leading to a charge separation between the free electrons and the ionic metal core and in turn the Coulomb repulsion among the free electrons acting as a restoring force pushes the free electrons to move in the opposite direction, which results in the collective oscillation of electrons or, in another words, the excitation of LSPR. The occurrence of LSPR also results in a strong absorption of light. MNPs of different sizes, shapes and materials show different absorption properties and thus may display different colors, such as is seen in the example in Fig. 1. Fig. 2(a) illustrates the excitation of LSPR for a spherical nanoparticle. Only one absorption band can be observed in its absorbance spectrum which is shown schematically in Fig. 2(b). For GNR, as demonstrated in Fig. 3(a) and (b), two absorption bands are evident in its absorbance spectrum, these being the longitudinal plasmon band (LPB) and the transverse plasmon band (TPB), corresponding as they do to electron oscillation along the long and the short axes of the GNR, respectively. The TPB of GNRs has been found to be insensitive to the changes in the size of the GNRs and the surrounding refractive index, whereas the LPB shows a red-shift with the increase of aspect ratio of GNRs and this is very sensitive to any change of the refractive index [20,26]. The properties of the LSPR are thus highly dependent on the size, shape and the dielectric property of the MNPs, as well as the nature of the local surrounding medium, as these factors affect the electron charge density on the particle surface [20,27–29]. LSPR is also highly sensitive to the refractive index change in the local dielectric environment. In many sensor schemes, the change of the peak wavelength or the peak absorbance in the absorption spectrum of MNPs is employed as an indicator of the LSPR sensor response [30,31].

As illustrated in Figs. 2 and 3, the excitation of LSPR results in a strong absorption of light. For spherical MNPs, the Mie solution to Maxwell's equations can be used to describe this light absorption caused by LSPR [32,33]. According to the Mie theory, for well separated spherical nanoparticles with a radius  $R$  (this being much smaller than the wavelength of light  $\lambda$  ( $R/\lambda < 0.1$ )), the extinction cross-section,  $C_{ext}$ , can be expressed as:

$$C_{ext} = \frac{24\pi^2 R^3 N \epsilon_m^{3/2}}{\lambda} \frac{\epsilon_i}{(\epsilon_r + 2\epsilon_m)^2 + \epsilon_i^2} \quad (1)$$

where  $\epsilon_m$  is the dielectric constant of the surrounding medium,  $\epsilon_r$  and  $\epsilon_i$  are the real and imaginary part of the dielectric function of the MNPs, respectively, and  $N$  is the number of spheres per unit volume. As indicated by Eq. (1), the plasmon absorption band appears when  $\epsilon_r = -2\epsilon_m$ . For gold and silver spherical nanoparticles, their plasmon absorption bands are located in the visible region, making these materials particularly suitable for many sensor applications where light from readily available sources such as lasers and LEDs is available.

Based on Mie theory, Zhong and co-workers simulated the LSPR bands of spherical gold nanoparticles of different sizes by using Eq. (1) [34]. Fig. 4(a) shows the simulated absorption spectra of GNSs of different diameters in aqueous solution. As shown in Fig. 4(a), one absorption band for each size of GNS can be observed in the simulated spectra and the absorption band shows a clear red shift

with increase in the size of the GNS. As demonstrated in Fig. 4(b), when they compared the simulated peak wavelengths of the LSPR absorption band of GNSs of different sizes with the results obtained in experiments, good agreement between the theoretical simulation data and the experimental data was found in the medium size range of GNSs, while slight divergence in the results were observed for both the smaller and the larger sizes [34].

In the case of metallic nanorods, Gans [35] predicted that for small ellipsoidal nanoparticles with dipole approximation, the surface plasmon mode would split into two distinct modes due to the surface curvature and geometry of the ellipsoidal nanoparticles. These small rods have commonly been treated as ellipsoids when explaining the optical properties of these rod-shape particles [36,37]. Therefore, Gans theory can be applied to describe the optical behavior of metallic nanorods and according to Gans' formula, the extinction cross-section  $C_{ext}$  for metallic nanorods can be calculated as follows [32,38,39]:

$$C_{ext} = \frac{2\pi V N \epsilon_m^{3/2}}{3\lambda} \sum_j \frac{(1/P_j^2)\epsilon_i}{(\epsilon_r + ((1-P_j)/P_j)\epsilon_m)^2 + \epsilon_i^2} \quad (2)$$

where  $V$  is volume of the particle and  $P_j$  is the depolarization factor. The depolarization factor for the elongated particles may be described as:

$$P_{length} = \frac{1-e^2}{e^2} \left[ \frac{1}{2e} \ln \left( \frac{1+e}{1-e} \right) - 1 \right] \quad (3)$$

$$P_{width} = \frac{1-P_{length}}{2} \quad (4)$$

where  $e$  is the ellipticity, given by:

$$e^2 = 1 - \left( \frac{length}{width} \right)^{-2} \quad (5)$$

where the relationship  $length/width$  is the aspect ratio of rod. The LSPR occurs when  $\epsilon_r = -((1-P_j)/P_j)\epsilon_m$ , where  $P_j = P_{width}$  for the longitudinal plasmon resonance and  $P_j = P_{length}$  for the transverse plasmon resonance. It is important to note that Eq. (2) also indicates that any small change in the aspect ratio of the nanorod will result in a significant change in the plasmon band, an important feature in sensor applications.

El-Sayed and co-workers reported the simulation of the absorption spectra of GNRs as a function of their aspect ratio, based on Gans theory [37]. Fig. 5(a) shows the simulated absorption spectra of GNRs of various aspect ratios in the medium with the same value of dielectric constant and using Eq. (2). As shown in Fig. 5(a), two LSPR bands of GNRs corresponding to TPB and LPB, as demonstrated in Fig. 3(b), can be observed in the simulated absorption spectra. It was found that the TPB has a small blue shift while the LPB has a large red shift with increasing aspect ratio of the GNRs. A linear relationship was also found between the peak wavelength of the LPB and the aspect ratio of the GNRs, which is in good agreement with the experimental data [37]. In addition, as demonstrated in Fig. 5(b), these authors also used Eq. (2) to simulate the absorption spectra of the GNRs with a constant aspect ratio, in a medium with varying dielectric constant. It can be observed in Fig. 5(b) that, although both the TPB and LPB show a red shift with increase of the dielectric constant of the surrounding medium, the LPB shift is much longer than that for the TPB, indicating that the LPB is more sensitive to the change of dielectric constant of the surrounding medium.

In addition, changes in the local medium surrounding the nanoparticles will result in a shift in the LSPR wavelength. This

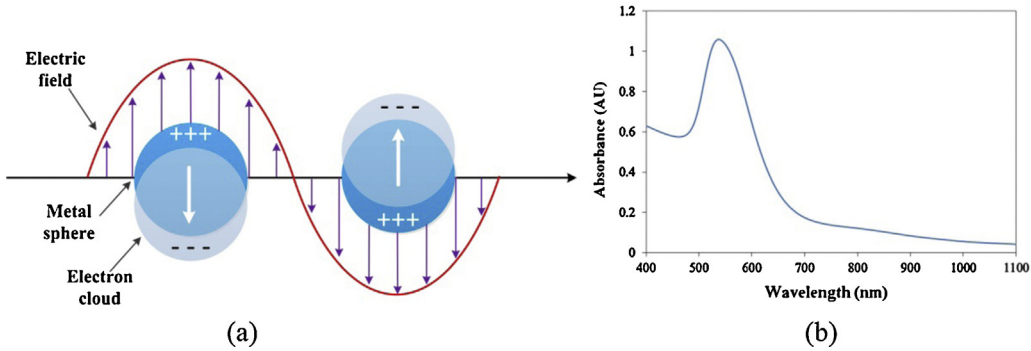


**Fig. 2.** (a) Schematic illustration of LSPR excitation for GNSs. Reproduced with permission from Ref. [14]. (b) A typical LSPR absorption band of GNSs.

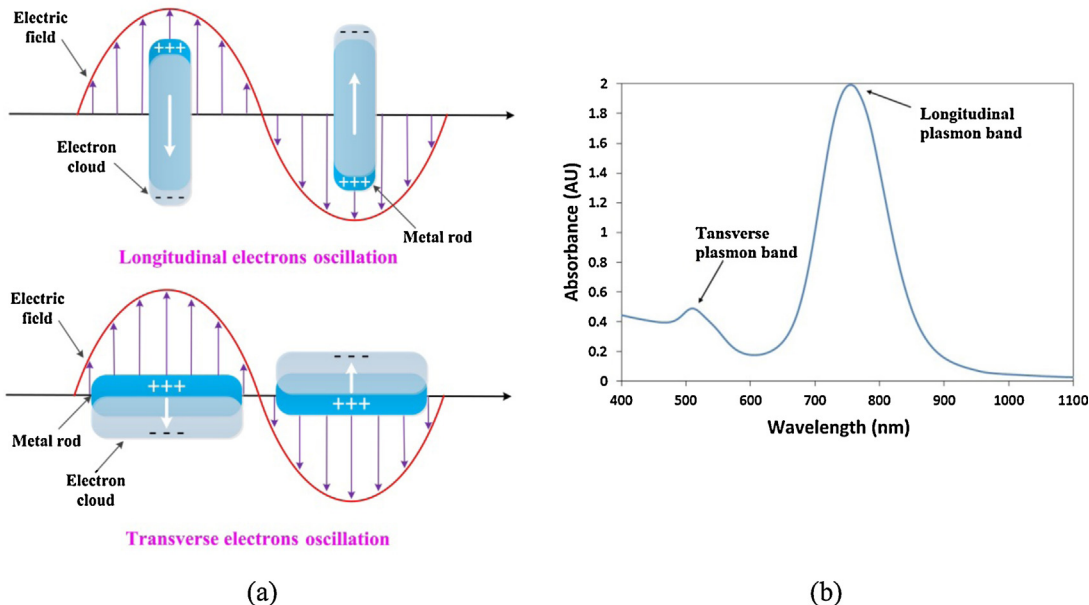


**Fig. 3.** (a) Schematic illustration of LSPR excitation for GNRs and (b) LSPR absorption bands of GNRs: longitudinal and transverse plasmon bands corresponding to the electron oscillation along the long axis (Fig. 3(a) top) and the short axis (Fig. 3(a) below) of GNR respectively.

LSPR wavelength shift,  $\Delta\lambda$ , seen in response to the refractive index change may be described by the following relationship [14,40,41]:

$$\Delta\lambda = m\Delta n \left[ 1 - \exp\left(\frac{-2d}{l_d}\right) \right] \quad (6)$$

where  $\Delta n$  is the change in refractive index (in refractive index unit, RIU),  $m$  is the bulk refractive index response of the nanoparticles

(and also known as the sensitivity factor, measured in nm per refractive index unit, nm/RIU),  $d$  is the effective thickness of the adsorbed layer (in nm) and  $l_d$  is the characteristic electromagnetic field decay length (in nm). The expression given in Eq. (6) forms a basis for LSPR wavelength-shift based sensors, in which the wavelength-shift due to the LSPR is used to monitor the refractive index change at the surface of nanoparticle. In sensor applications

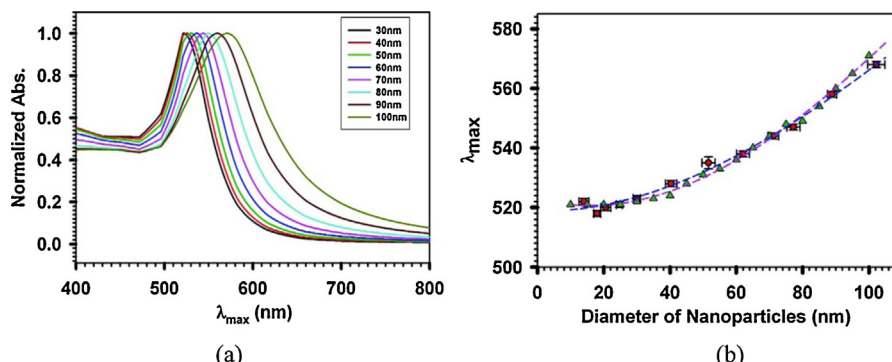


**Fig. 4.** (a) Simulated LSPR absorption spectra (normalized) of GNSs with different diameters in aqueous solution and (b) comparison between the simulation data and the experimental data for the peak wavelength of LSPR absorption band vs. diameter of GNSs. Triangles and circles present the simulation data and the experimental data, respectively.

Reprinted with permission from Ref. [34].

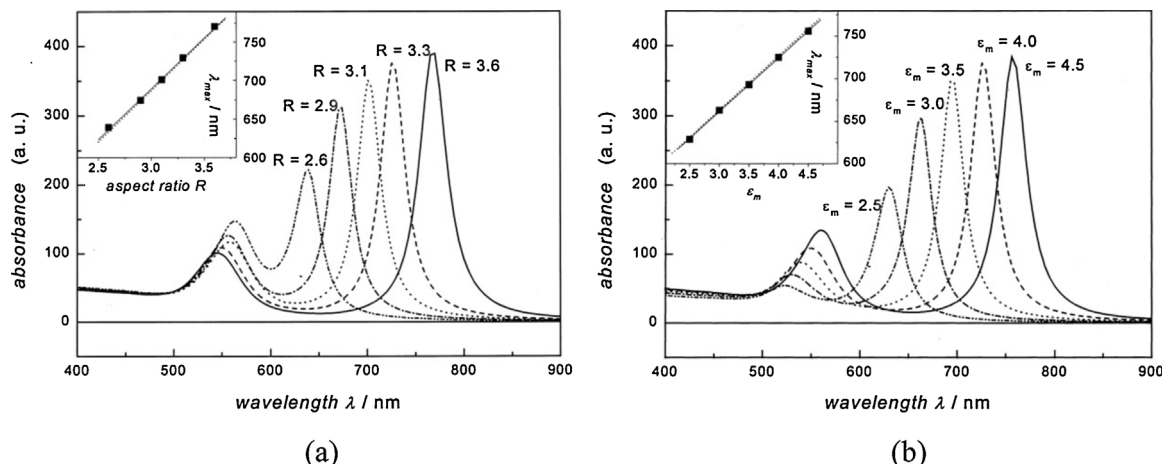


**Fig. 5.** (a) Simulated LSPR absorption spectra of GNRs with various aspect ratios in the medium with a constant dielectric constant (inset: peak wavelength of LPB increases linearly with aspect ratio of GNRs); (b) simulated LSPR absorption spectra of GNRs with a constant aspect ratio in the medium with varying dielectric constant (inset: peak wavelength of LPB increases linearly with dielectric constant of the surrounding medium).

Reprinted with permission from Ref. [37].

this may be due, for example, to the adherence of biomolecules. For GNRs, as LPB seen with GNRs is more sensitive to the refractive index change, the parameter  $\Delta\lambda$  (in Eq. (6)) represents the peak wavelength shift of the LPB.

### 3. Synthesis of GNRs

The successful development of LSPR sensors using GNRs depends on the reliable and accurate synthesis of GNRs that can then be applied to create consistent and reproducible sensors. The history of synthesis of spherical gold nanoparticles dates back more than a century. The most commonly used method for producing GNSs is citrate reduction, where the GNSs are synthesized by the addition into the boiling gold salt ( $\text{HAuCl}_4$ ) solution of a known amount of citrate solution, allowing the size of GNSs to be easily controlled by adjusting the ratio between the citrate and the gold salt [42–44]. However, the synthesis of the GNRs appears more complicated, and the successful and reliable synthesis of GNRs was achieved only in the past decade. Fortunately, the unique and thus very interesting optical properties of GNRs have focused the attention of many researchers who have devoted their efforts to the synthesis of GNRs. There are several common methods have been developed and applied for synthesizing GNRs and reported in the literature, and in this section, a brief review of several typical synthesis methods is discussed.

#### 3.1. Seed-mediated growth method

Among the various GNRs synthesis methods reported, the seed-mediated growth method is the most popular and this has been widely applied due to the simplicity of the experimental procedure, the high yield of nanorods of high quality, the ease of particle size control and the flexibility in structural modifications [20]. The seed-mediated growth approach for colloidal GNRs was first demonstrated by Jana et al. in 2001 [45]. In their work, the seed solution was prepared by the reduction of gold salt ( $\text{HAuCl}_4$ ) with  $\text{NaBH}_4$  in the presence of sodium citrate, which resulted in the formation of citrate-capped GNSs with a diameter of about 3–4 nm and used as the seeds. Following that, the seed solution was added to a growth solution containing  $\text{HAuCl}_4$ , cetyl-trimethyl ammonium bromide (CTAB, as the template), ascorbic acid (as the reducing agent) and  $\text{AgNO}_3$  (for shape induction) to allow the growth of GNRs to occur. As a result, GNRs with various aspect ratios were created by adding different volumes of seed solution to

the different samples of the growth solution, as shown in Fig. 6. In later work, this group also modified the method described by introducing a three-step protocol (in the absence of silver ions) to grow GNRs with a higher aspect ratio, in this case being up to 25 [46]. In this three-step method, the seed solution and the growth solution were prepared following a similar procedure used in preparing the short GNRs, but without the addition of  $\text{AgNO}_3$ . Then, at Step one, the seed solution was added to the growth solution (in this case to form small GNRs), with these being used subsequently as the seeds which were added to the growth solution to create bigger GNRs, at this Step two. The final step (Step three) is undertaken by adding the bigger GNRs developed to the growth solution, to create the desired GNRs, in this case with a higher aspect ratio. However, the biggest drawback of this method is that, apart from the GNRs, a large amount of GNSs as well as particles with other shapes are also produced as by-products and this effect significantly alters the overall shape of the plasmon absorption bands of the GNRs and thus requires time-consuming multiple rounds of centrifugation to purify the GNR solution thus produced [20].

In 2003, research carried out by Nikoobakht and El-Sayed created a significant improvement to the above method by introducing two important modifications: first, they replaced the sodium citrate that was originally used with CTAB, this being a stronger stabilizer, in the seed formation step and second, they adjusted the amount of silver ions in the growth solution to control the aspect ratio of the GNRs formed [47]. In their work, the seed solution was prepared by reducing  $\text{HAuCl}_4$  in the presence of the CTAB surfactant with ice-cold  $\text{NaBH}_4$ . The growth solution was prepared by mixing  $\text{HAuCl}_4$  and a known volume of  $\text{AgNO}_3$  solution in the presence of CTAB, followed by the addition of ascorbic acid. In this way, the GNRs start to grow directly after the addition of seed solution in the growth solution. Using this method, a yield as high as 99% for the GNRs (with aspect ratios from 1.5 to 4.7) was achieved. To synthesize GNRs with even higher aspect ratios, a co-surfactant, benzylidimethylhexadecylammonium chloride (BDAC) was introduced in the original growth solution. By adjusting the concentration of silver ions in the growth solution, GNRs with aspect ratios up to 10 had been synthesized [47]. Due to the high quality and yield of GNRs produced, the method reported by Nikoobakht and El-Sayed has been widely applied for synthesizing GNRs for sensor applications.

More recently, Murray and co-workers reported an improved synthesis of GNRs through a technique using seed-mediated growth and employing aromatic additives and a low CTAB

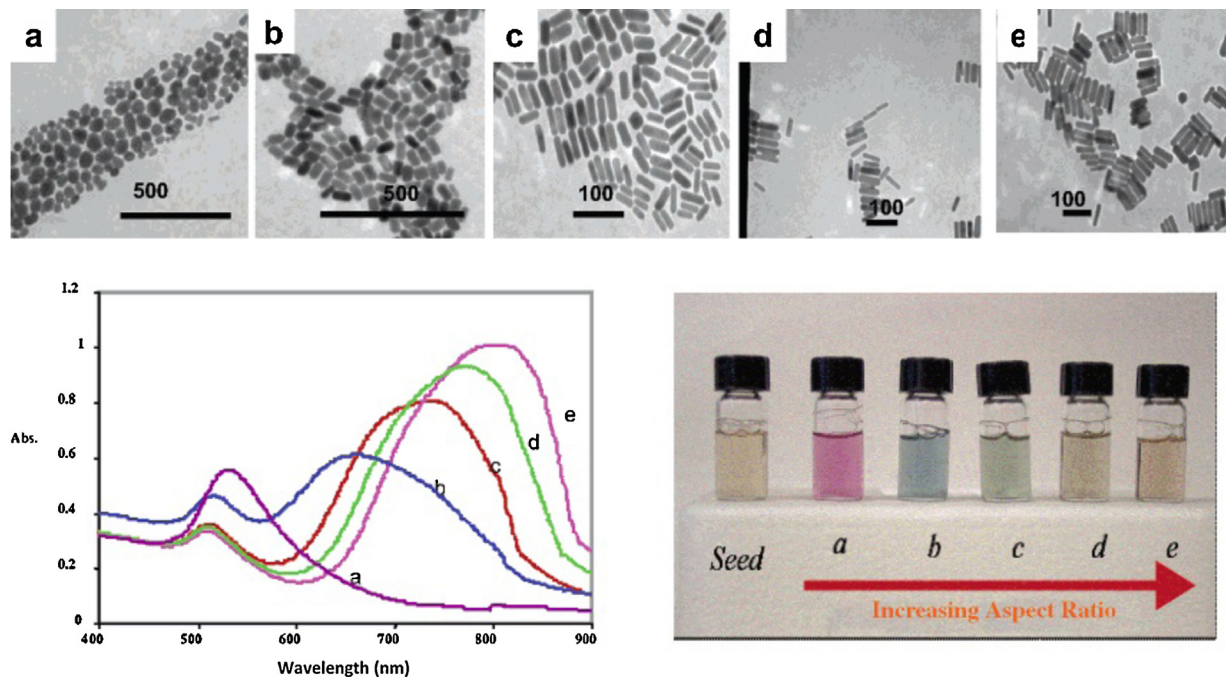


**Fig. 6.** TEM images (top), absorbance spectra (left) and photographs (right) of aqueous solutions of GNRs with various aspect ratios ranging from: (a)  $1.35 \pm 0.32$ , (b)  $1.95 \pm 0.34$ , (c)  $3.06 \pm 0.28$ , (d)  $3.50 \pm 0.29$ , (e)  $4.42 \pm 0.24$ .

Reprinted with permission from Ref. [49].

concentration [48]. This approach was shown to produce GNRs with a broad LPB tuneable range but a lower level of impurities, as demonstrated in Fig. 7. In their work, the seed solution was prepared following the same procedure as reported by Nikoobakht and El-Sayed [47]. However, when preparing growth solutions, an appropriate amount of salicylate-based sodium salts was added to grow short GNRs with LPB less than 700 nm, while organic acid additives were added to growth solutions to synthesize longer GNRs with LPB greater than 700 nm. In both cases, the concentration of the CTAB in growth solution was reduced from the value of 0.1 M which was applied in the original approach to 0.05 M. The addition of aromatic additives has an effect on the micellar structure of CTAB to increases the chance of forming GNRs. The aspect ratio of the GNRs was controlled by adjusting the concentration of the silver ions and the amount of seed solution used. The results showed that the GNRs synthesized through the method described were of high mono-dispersion, with a shape impurity of less than 1% and a broad LPB which was tunable over the wavelength range from 627 to 1246 nm [48].

Despite the high yield of GNRs produced, the seed-mediated growth method is a delicate approach to implement in which the variation in many different parameters, such as the concentration of the seed solution, the aging time, the temperature, pH and the concentration of CTAB solution will lead to significant differences in parameters such as the shape, aspect ratio and yield as well as the absorption band of GNRs, this seriously affecting the final formation of GNRs [20,49–53]. It has been found that even the fact that the CTAB surfactant was purchased from different suppliers (although nominally the same) also affects the aspect ratio and the yield of the GNRs, due the impurity of the different CTAB surfactants [54]. Therefore, it is important to keep all these critical parameters the same from one experiment to another, in order to obtain consistent results.

### 3.2. Electrochemical method

Despite the fact that the seed-mediated growth method has become a common approach for synthesizing GNRs, the

preparation of high yield of GNRs was actually first demonstrated by using an electrochemical method, this being seen as the precursor of the seed-mediated growth method [55,56]. In the 1990s, Wang and co-workers first reported the formation of GNRs by extending their previous work on electrochemical synthesis of metal clusters in the reversed micelles in an organic solvent. The synthesis of GNRs is conducted within a two-electrode-type electrochemical cell, as shown in Fig. 8(a), where a gold metal plate was used as the sacrificial anode and a platinum plate cathode was immersed into the electrolytic solution containing a rod-inducting cationic surfactant CTAB and a cationic co-surfactant tetradodecylammonium bromide (TCAB). Small amounts of acetone and cyclohexane were also added into the electrolytic solution before the electrolysis. Acetone was used for loosening the micellar framework and cyclohexane was necessary to enhance the formation of elongated rod-like CTAB micelles [56]. During the electrolysis, the bulk gold metal anode was consumed to form  $\text{AuBr}_4^-$ , which then complexes with the cationic surfactants and migrates to the cathode, where the reduction occurs. Ultrasonication was needed to dissipate the GNRs and keep them away from the cathode during the electrolysis. The aspect ratio of the GNRs was controlled by gradually immersing a silver plate in a position behind the platinum cathode. It had been found that the aspect ratio of the GNRs was influenced both by the concentration and the release rate of the silver ions produced from the redox reaction between the gold ions generated from the anode and the silver plate. However, the synthesis mechanism, as well as the role of the silver ions, is still not fully known.

### 3.3. Template method

The template method is based on the electrochemical deposition of gold within the pores of nanoporous ion-track etched polycarbonate or alumina membrane template. This method was initially used for the preparation of microscopic electrodes [57] and Martin and co-workers first employed the template method to synthesize GNRs [36,58,59]. The template was prepared by

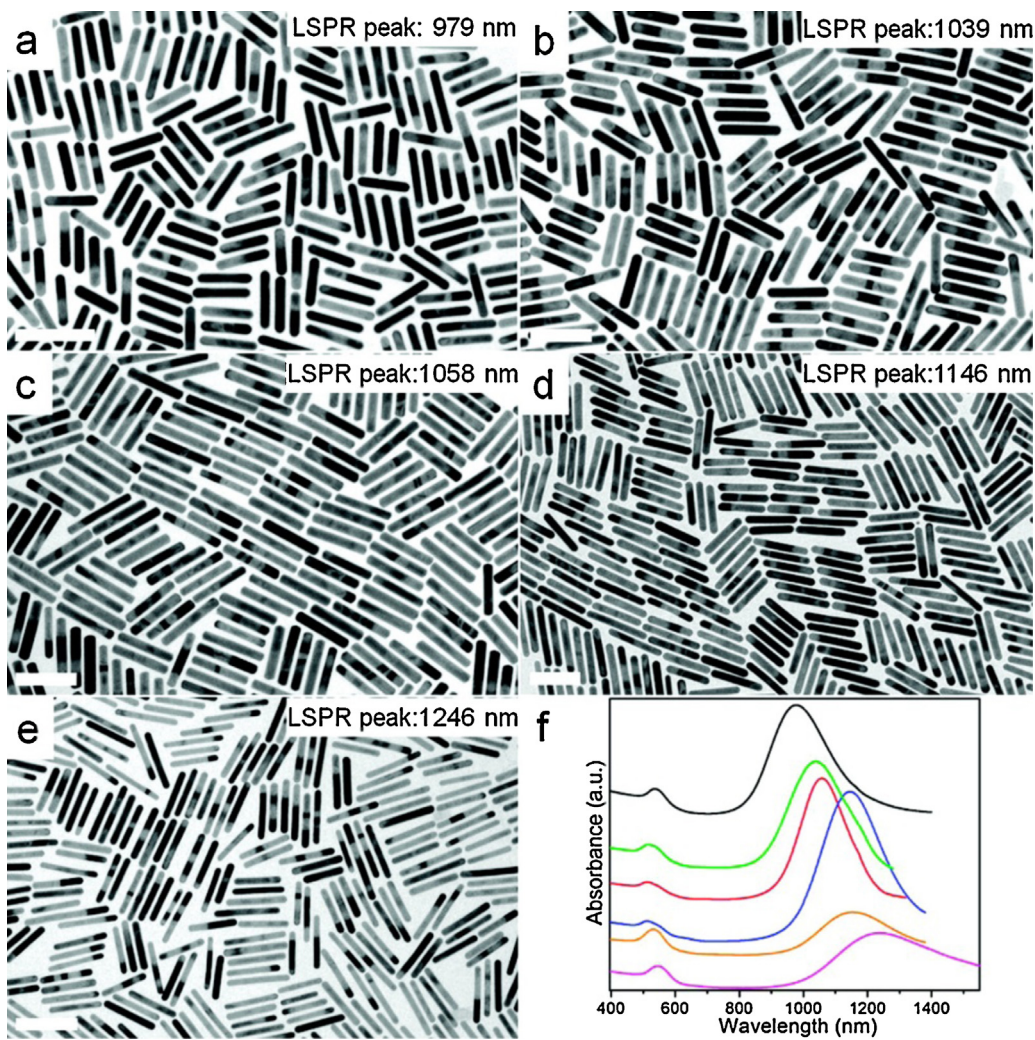


**Fig. 7.** Effect of an improved synthesis of GNRs using aromatic additives. (a)–(e) TEM images of as-synthesized GNRs with different aspect ratios and LPB wavelengths, (f) the corresponding absorption spectra of GNRs in (a)–(e) with black, green, red, blue, and magenta curves, respectively. (For interpretation of the references to color in this figure legend, the reader is referred to the web version of this article.)

Reprinted with permission from Ref. [48].

anodization of aluminum in an acidic solution, which resulted in the formation of uniform pores with diameters of 5–200 nm in the aluminium template where the pore length was seen to be dependent on the anodization time. The GNRs were formed through an electrochemical deposition of gold into the template pores within an electrochemical cell, followed by the chemical etching of the aluminium template to release the synthesized GNRs. Fig. 9(a) and (b) shows the alumina membrane template and the synthesized GNRs with different aspect ratios, respectively. The width of the rods created coincides with the diameter of the pores and the length of the rods could be controlled by varying the amount of the gold deposited within the pores of the template [60]. The disadvantages of the template method are reported to include a variance in the length of the GNRs formed, due to the uneven deposition of gold and further a low yield of GNRs [21,61].

#### 3.4. Electron beam lithography method

Electron beam lithography (EBL) is a lithographic technique commonly used in the generation of metallic nanostructures, where this technique allows for the precise control of the size, shape and the spatial distribution of the nanoparticles formed [62]. Fig. 10(a) illustrates the procedure for the fabrication of the gold

nanoparticles using the EBL method. In this an electron-sensitive photoresist, such as poly(methyl methacrylate), PMMA, was coated over a glass slide which was covered by a conductive film such as indium tin oxide (ITO). The PMMA coated glass slide was then exposed to an electron beam to form the desired pattern on the PMMA film. A chemical developing agent was then applied to selectively remove the electron beam exposed polymer segment, followed by the deposition of gold in the patterns by thermal evaporation. The unexposed PMMA film resulting, as well as the gold film deposited on it, was finally removed by using acetone that leaves the desired gold nanoparticle arrays on the glass slide [63], as shown in Fig. 10(b). The disadvantages of this technique involve it being a time-consuming process with a low yield of nanoparticles at any one time, due to the small size of the producing region [32].

#### 3.5. Other methods

Yang and co-workers have reported the synthesis of synthesized colloidal GNRs using a photochemical method [64]. In their work, the GNRs were formed by using UV light from a lamp at 254 nm to irradiate a growth solution consisting of gold salt, CTAB and TCAB surfactants, silver nitrate, acetone and hexane, for more than 24 h. The UV light works as a reducing agent, operating similar to

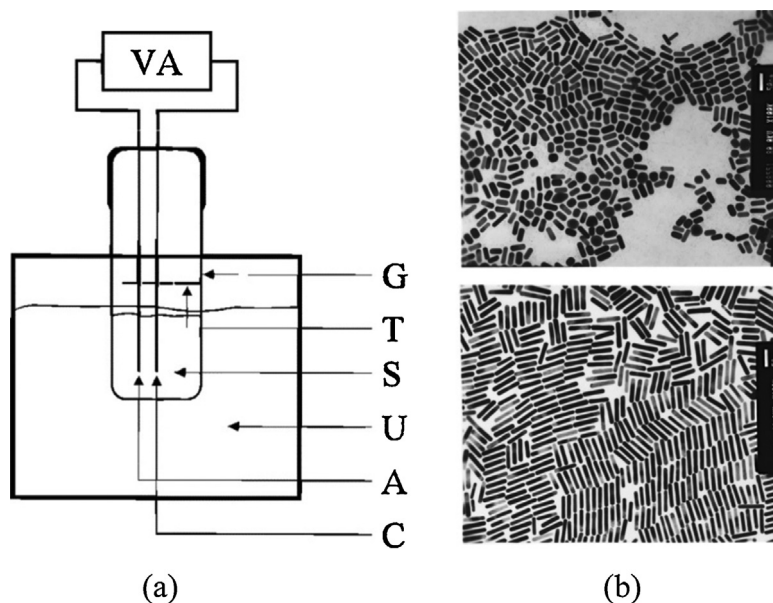


**Fig. 8.** (a) Schematic diagram of the set-up for electrochemical synthesis of GNRs containing: VA, power supply; G, glassware electrochemical cell; T, Teflon spacer and the electrode holder; S, electrolytic solution; U, ultrasonic cleaner; A, anode (Au); C, cathode (Pt). (b) TEM images of Au nanorods with two different mean aspect ratios: 2.7 (top) and 6.1 (bottom).

Reprinted with permission from Ref. [56].

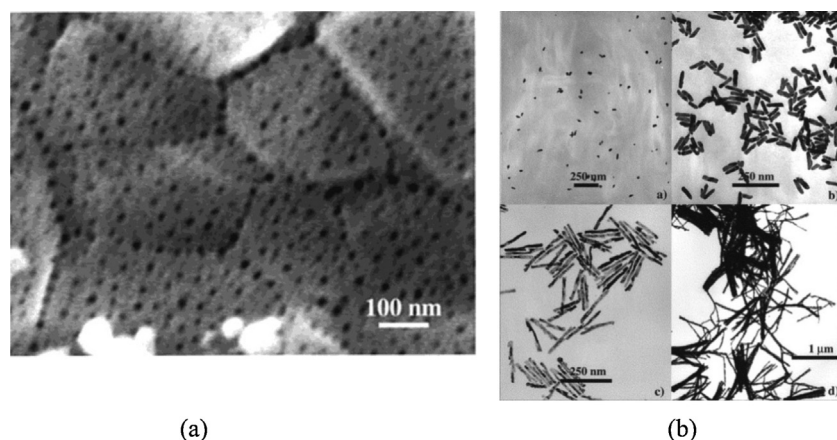


**Fig. 9.** (a) FEG-SEM image of the alumina membrane template and (b) TEM images of GNRs obtained by the template method. Reprinted with permission from Ref. [60].

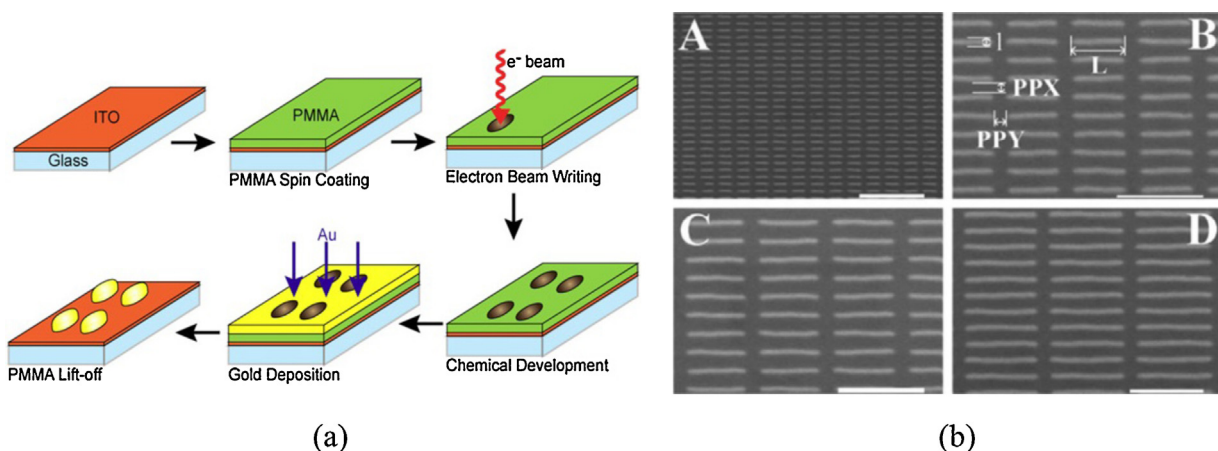


**Fig. 10.** (a) Schematic diagram of the fabrication of gold nanoparticles using EBL. Reprinted with permission from Ref. [32]. (b) SEM images of GNRs arrays produced by EBL. All of the rods have widths,  $l$ , of 60 nm, heights of 50 nm, and lengths,  $L$ , of (A) 420 nm, (B) 620 nm, (C) 720 nm, and (D) 1  $\mu$ m. Reprinted with permission from Ref. [63].

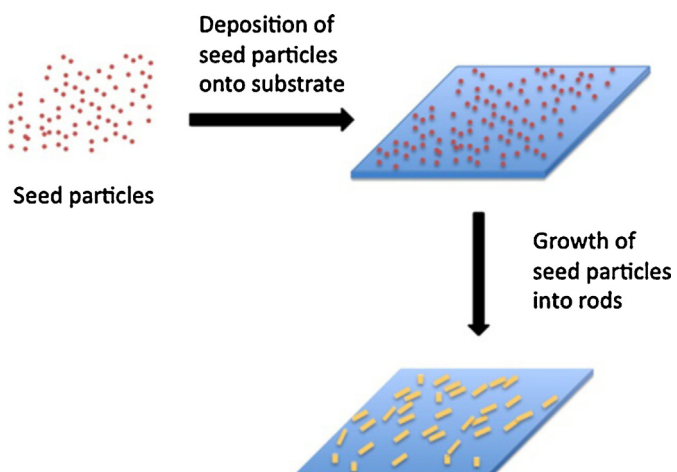


**Fig. 11.** Schematic diagram of the process of direct growth of GNRs on the substrate surface.

Reprinted with permission from Ref. [72].

the role of ascorbic acid in the seed-mediated growth method, to convert  $\text{Au}^{3+}$  to  $\text{Au}^0$ . The aspect ratio of the GNRs thus produced could be controlled by varying the concentration of the silver ions in the growth solution, leading to the corresponding LSPR plasmon bands, located at wavelengths between 600 and 800 nm. It was found possible to extend the aspect ratio of the GNRs formed by applying light from a 300 nm UV source instead and thus allowing the synthesizing time to be shortened by increasing the optical intensity [65]. Taub et al. developed a method that enables the GNRs directly to grow on various substrates [66] by adapting the seed-mediated growth method proposed by Jana and co-workers [46]. As demonstrated in Fig. 11, the spherical seed nanoparticles were first immobilized on the surface of a mica substrate by a dip coating method, followed by immersing the seed-coated substrate into the growth solution, to allow the GNRs to directly grow on the substrate surface. However, it was found that only 15% of the seeds attached to the mica surface were found to grow as nanorods [66]. In addition, other less popular methods for the preparation of GNRs have also been reported, such as proton beam irradiation [67], bioreduction [68], microwave reduction [69] and solvothermal reduction [70].

#### 4. Surface modification of the CTAB-capped GNRs

For GNRs synthesized in the presence of a CTAB surfactant using the wet-chemical methods, such as the seed-mediated growth method and electrochemical method, the surface of these GNRs is covered by a bilayer of positively charged CTAB molecules, as illustrated in Fig. 12. The CTAB surfactant is important to the synthesis of GNRs, because it not only works as a “structure-directing agent” to control the final particle shape, but also acts as a stabilizer to protect

the as-synthesized GNRs against aggregation [71,72]. This is similar to the citrate-capped GNSs synthesized through citrate reduction, as citrate here works both as a reducing agent and a stabilizer to prevent the aggregation of GNSs [73]. However the difference is that the citrate-capped GNSs are highly stable in aqueous solution with a neutral pH value and therefore, they can be readily used for further functionalization with biomolecules, such as DNA, for LSPR biosensing [74,75]. However, the CTAB-capped GNRs are only stable when suspended in a CTAB aqueous solution with a lower pH value and the stability has been found to become less satisfactory under several different conditions, such as where there is a high salt content, a low CTAB concentration and for the addition of organic solvents, thus limiting the further applications of GNRs [76,77]. In addition, it also has been found in in vitro studies that the free CTAB molecules are cytotoxic to human cells, while the CTAB molecules bound to the GNRs surface are not toxic [78]. Despite the fact that most of the free CTAB can be removed by centrifugation, the complete removal of the free CTAB in solution as well as the CTAB attached to the GNRs will result in a serious aggregation and deposition of GNRs. Therefore, it is necessary to modify the surface conditions of CTAB-capped GNRs in order to extend their applications, for example, for biosensing, biomedical imaging and drug delivery [20,24]. So far, various approaches have been proposed for such a surface modification of CTAB-capped GNRs and, in general, there are two strategies applied for this purpose: surface covering and ligand exchange.

##### 4.1. Surface covering

This approach aims to introduce an additional coating to cover the entire surface of the CTAB-capped GNRs. An easy way of doing this is to coat the positively charged surface of the GNRs covered by CTAB molecules with anionic polyelectrolytes through the use of electrostatic absorption and for example, poly(sodium-4-styrenesulfonate) (PSS) has been applied to coat the GNRs. The anionic PSS not only switches the positive surface charge of GNRs to negative, but also enables antibodies to attach to the GNRs, via hydrophobic interactions [24,79]. Poly(acrylic acid)(PAA) is another anionic polyelectrolyte applied to create this coating for GNRs. The carboxylic group of PAA allows the proteins and amine-terminated biomolecules to be covalently bound to the PAA modified GNRs via an EDC/NHS coupling reaction [80]. In addition, Gole and Murphy in their work have reported a layer-by-layer (LBL) technique which can be used to manipulate the surface condition of GNRs, and make them suitable for a range of different applications [81]. As shown in Fig. 13(a), the anionic PSS and cationic poly(diallyldimethylammonium chloride) (PDADMAC) are alternately deposited onto the CTAB-capped GNRs and multilayers of coating can be obtained by repeating the cycle. This polyelectrolyte coating method is easy and fast, but the stability of the coating obtained through electrostatic interaction is in question for long-term storage or for in vivo applications [20].

Surface modification of GNRs with a coating of hard inorganic materials, such as silver and silica, has also been achieved. Ah et al. have reported the deposition of the silver layer on the surface of CTAB-capped GNRs by reducing the silver chloride solution with hydroxylamine, in the presence of GNRs [82]. The deposition of the silver coating forms an Au/Ag core/shell structure of GNRs and the thickness of the silver shell can be controlled by adjusting the concentrations of the silver chloride and hydroxylamine used. The silver shell can also be removed by using hydrochloric acid to restore the GNRs. In later work, Liu and Guyot-Sionnest have proposed a slightly different method for coating CTAB-capped GNRs with silver [53]. In their research, the deposition of the silver coating was achieved by the reduction of the silver nitrate with ascorbic acid in the presence of a GNR solution and stabilizing agent, using

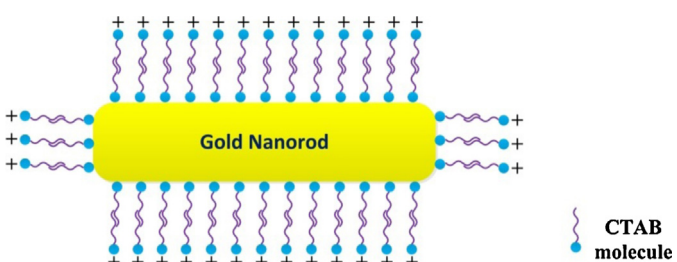


**Fig. 12.** A schematic of a gold nanorod covered by a bilayer of positively charged CTAB molecules.

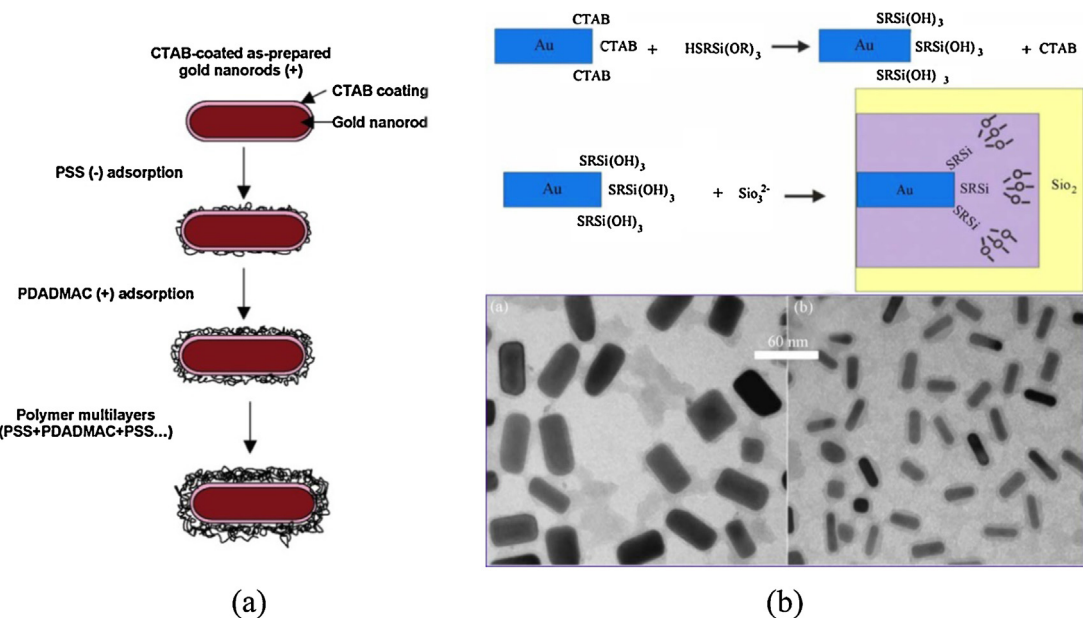


**Fig. 13.** (a) Surface modification of CTAB-capped GNRs with polyelectrolytes using LBL technique. Reprinted with permission from Ref. [81]. (b) Top: scheme showing the steps required for silica coating of GNRs. Bottom: TEM images of silica coated GNRs with different aspect ratios (a – 1.94; b – 3.08). Reprinted with permission from Ref. [39].

either citrate or polyvinylpyrrolidone (PVP). It was also found that the pH of the coating solution has an impact on the deposition rate of the silver where the higher the pH, the higher the deposition rate achieved [83]. The Au/Ag core/shell nanorods are more stable and show sharper, stronger and blue-shifted surface plasmon absorption bands than do the original GNRs [53,82].

In an approach which is similar to the silver coating, a method initially developed by Liz-Marzán et al. for the silica coating of citrate stabilized spherical gold nanoparticles [84] has been applied for the deposition of a silica coating onto the surface of CTAB-capped GNRs to form an Au/silica core/shell structure [85,86]. As demonstrated in Fig. 13(b), the silica coating is formed by simply adding sodium silicate solution to a premixed solution consisting of GNRs solution and 3-mercaptopropyl trimethoxysilane (MPTMS) or 3-mercaptopropyl triethoxysilane (MPTES) solution and the formation of the silica shell results in a red-shift of the longitudinal plasmon band of the GNRs due to the refractive index change at GNRs surface. Using a further approach, the silica has also been successfully coated on the GNRs by the injection of tetraethoxysilane (TEOS) to the CTAB-capped GNRs solution (in the basic condition) which enables thin and highly porous silica shells to create a covering for the GNRs [87]. The silica coating allows the GNRs to be modified with silane coupling agents for further functionalization and then transfer to organic solvents [20].

#### 4.2. Ligand exchange

Another common strategy for GNR surface modification is to replace the attached CTAB bilayers with thiol-terminated ligands which are then firmly bound to the GNRs surface via the strong Au–S covalent bonds, as illustrated schematically in Fig. 14(a). The advantages of this method include the reduction of the cytotoxicity of GNRs due to the removal of the CTAB molecules and the increase of the biocompatibility of GNRs when ligands with functional groups are applied. However, as this method involves the removal of the CTAB molecule, the chance of the GNRs aggregation will also increase due to the loss of protection of CTAB. Therefore, strict control of the experimental conditions are routinely required to prevent the GNRs from aggregating during the modification process. The thiol-terminated polyethyleneglycol (PEG) is one of

the popular ligands commonly used for GNR surface modification [88–91] where one advantage of using thiolated PEG is that PEG is a water-soluble polymer so that the modification of GNRs can be conducted in an aqueous condition. The ligand exchange takes place after the addition of the thiolated PEG solution to the centrifuged GNR solution, with the mixture being kept under constant stirring and followed by 3 days of dialysis or several rounds of centrifugation to remove the excess CTAB and PEG. Such PEG-modified GNRs are highly stable in aqueous and some even in organic solutions, and are useful in in vivo applications such as biomedical imaging and photothermal therapy [21,91]. In addition, by employing the

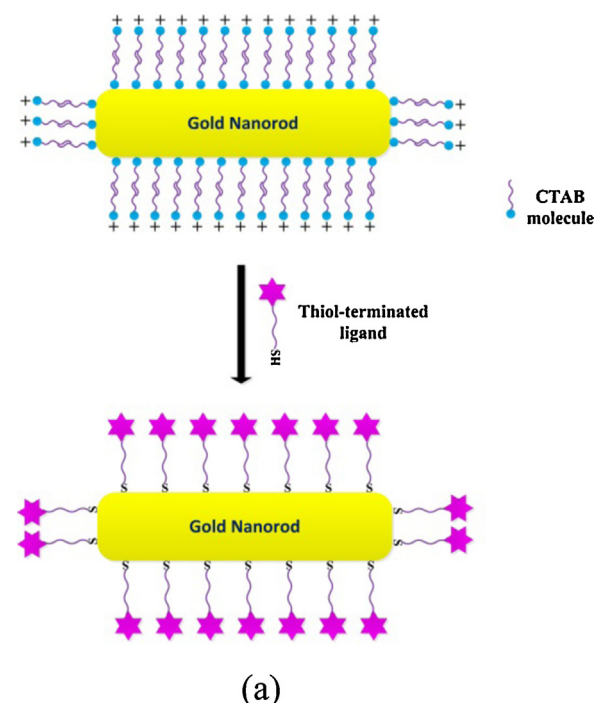


**Fig. 14.** Schematic illustration of the surface modification of CTAB-capped GNRs with thiol-terminated ligands.

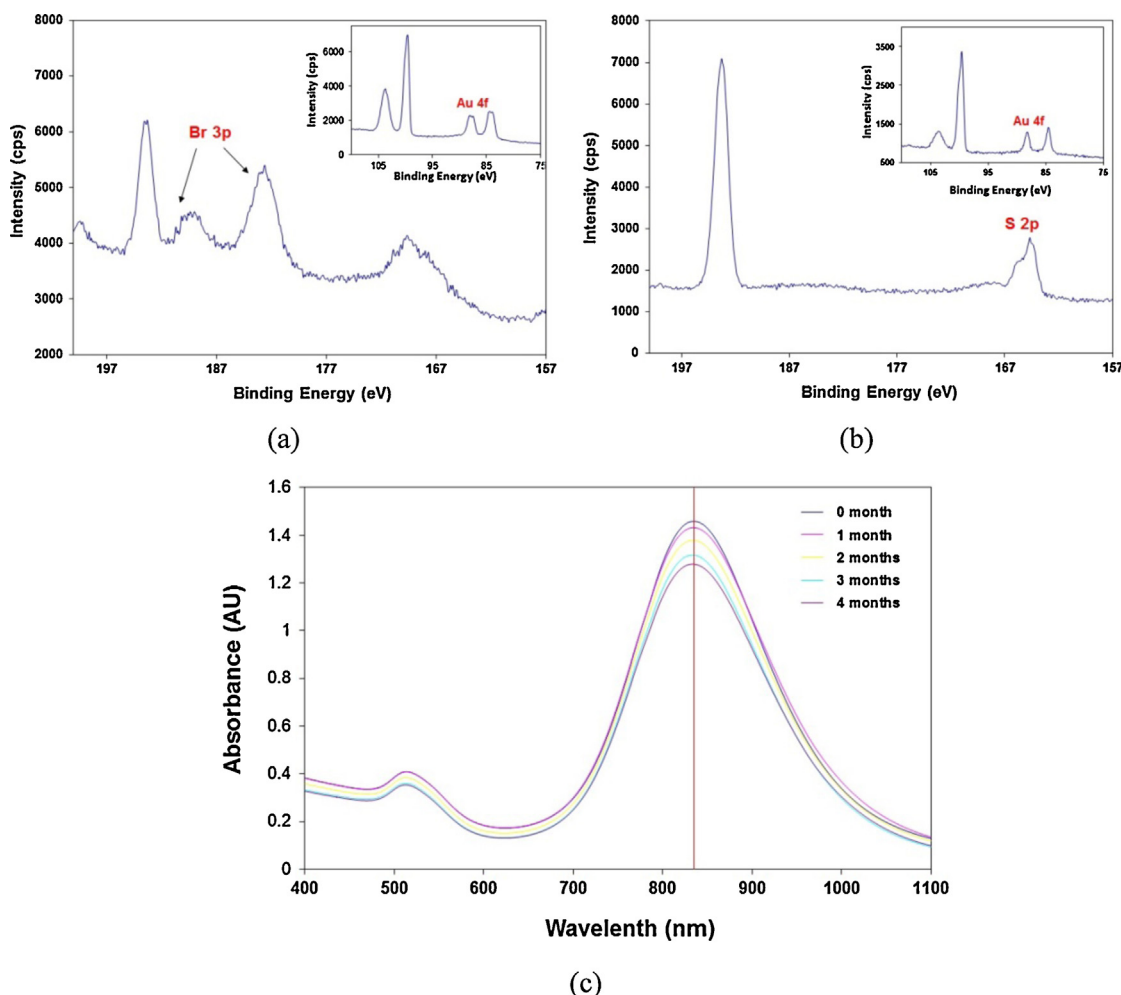


**Fig. 15.** XPS spectra of (a) CTAB-capped GNRs, and (b) MUA-modified GNRs; (c) Absorption spectra of MUA-modified GNRs in borate buffer at pH 9 during 4 months storage at 4 °C.

Reprinted with permission from Ref. [96].

thiolated PEGs with biofunctional groups, it is also possible to bind the biomolecules such as proteins and antibodies to the PEG-modified GNR surface [76,92]. However, the large size of the thiolated PEGs makes it difficult for them to reach the GNR surface due to the dense CTAB bilayer and this will result in an incomplete removal of CTAB molecules. Further, the large size of the thiolated PEGs also increases the distance between the analytes and the PEG-modified GNR surface, which will reduce the sensitivity when they are used as LSPR biosensors [93]. Therefore, small thiol-terminated ligands such as 11-mercaptopoundecaonic acid (MUA) and cysteamine normally are preferable for complete removal of CTAB [20].

The surface modification of the GNRs with MUA has been reported in several reported studies [93–95]. The MUA molecule has a carboxylic group which is desirable for bioconjugation with amine-terminated biomolecules, such as proteins and antibodies. Therefore, once the MUA molecules are bound to the GNRs surface, without further functionalization biomolecules can be conveniently attached on to the GNRs via EDC/NHS coupling. However, like most thiol molecules, MUA is not water-soluble and it only dissolves in organic solvents such as ethanol and chloroform. The hydrophobic nature of the MUA creates a major challenge to the surface modification of GNRs with MUA because the CTAB-capped GNRs are very unstable in the presence of organic solvents and this will cause an irreversible aggregation of GNRs. Several approaches have been proposed in order to enable the MUA to be applied in

the surfaced modification of GNRs. Yu *et al.* have reported a method for complete removal of CTAB on GNRs with MUA [93]. The ligand exchange was conducted by adding a MUA-ethanol solution to a centrifuged GNRs solution under constant ultrasonication to prevent the GNRs from aggregating. The temperature of the mixed solution was also elevated to 50 °C to release the CTAB molecules from the GNR surface and then brought back to room temperature. The GNRs were finally purified through centrifugation. Although such MUA-modified GNRs have been proven by the authors to be suitable for use as LSPR biosensor probes, significant aggregation of the GNRs was observed by ourselves (as well as by other researchers) by following the procedure reported, indicating that this method requires strict experimental conditions which makes it difficult as a method for practical use. Thierry and co-workers later modified this method using a two-step strategy [94]. They first used the thiolated PEG to replace the majority of the CTAB molecules on the GNR surface in an aqueous condition. The PEG-modified GNRs have a neutral charge on the GNR surface to prevent them from aggregating in organic solvents as readily as do the positively charged CTAB-capped GNRs. The second step involved the replacement of the PEG with MUA following a similar procedure to that applied in the work of Yu *et al.* Although this approach may avoid the massive aggregation of GNRs, as observed in the work of Yu *et al.*, the thiolated PEG molecules were also bound to the GNRs via the strong Au–S bonds as MUA and whether MUA is able to effectively replace the PEG is still questionable for this route. In another

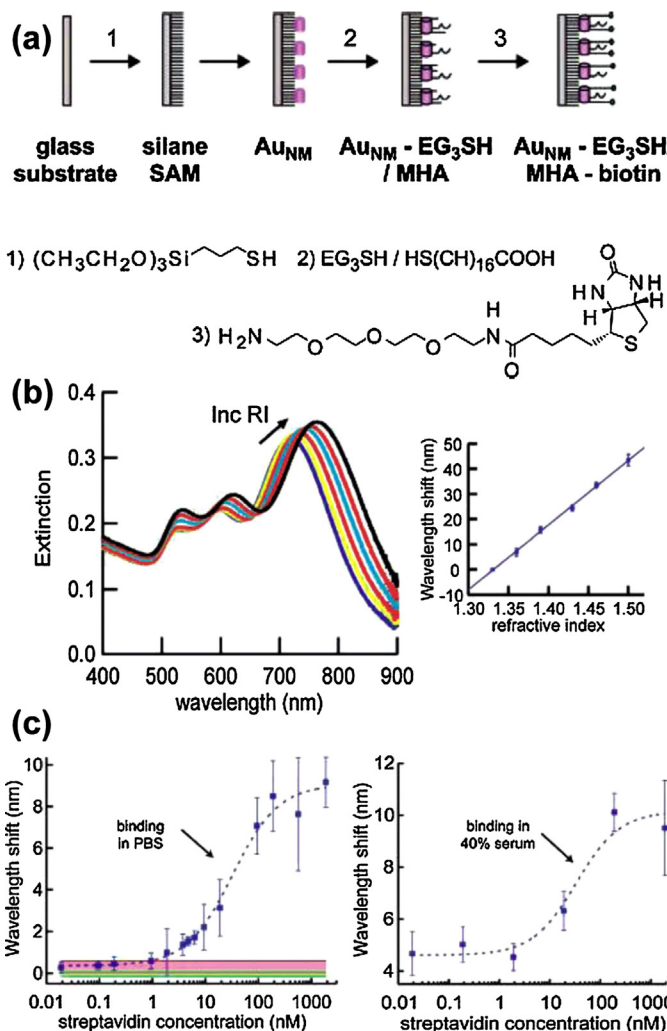


**Fig. 16.** Illustration of GNR refractive index sensing. (a) Schematic of the sensor construction. GNRs are first immobilized onto a thiolated glass substrate, then modified with a biotin-terminated self-assembled monolayer. (b) Extinction spectra of GNR-based LSPR sensor with increase of refractive index (left) and measurement of refractive index sensitivity (right). (c) LSPR sensor response for biotin-streptavidin binding in PBS (left) and 40% serum (right). Adapted with permission from Ref. [15].

study reported by Dai et al., to prevent the irreversible aggregation of GNRS, the surface modification with MUA was conducted inside an ionic exchange resin [95]. The CTAB-capped GNRs were first loaded into the polymer resin beads suspended in an aqueous solution to “trap” the GNRs in the resin beads. The ligand exchange took place after the addition of the MUA chloroform solution to the resin beads suspension and the MUA-modified GNRs diffused out of the beads into the chloroform solution. The resin beads applied in this work can effectively prevent the GNRs from aggregating during the reaction. This approach is both elegant and effective but, however, it also appears to be time consuming and complex to operate [94].

Recently, in work by the authors, a simple yet robust pH-mediated method for effectively modifying the surface of CTAB-capped GNRs synthesized through seed-mediated growth was reported [96]. This method allows the complete replacement of the CTAB molecules attached on the GNRs surface with the MUA molecules to take place in a total aqueous environment, by controlling the pH of the MUA aqueous solution, thus avoiding the irreversible aggregation of GNRs during the complex surface modification process observed in the previous reported methods. The success of the complete replacement of CTAB with MUA was confirmed with surface elemental analysis using an X-ray

photoelectron spectroscopy (XPS), as shown schematically in Fig. 15(a), and the MUA-modified GNRs created in this work has demonstrated a high stability, over a period of up to 4 months at least, when stored in a buffer solution at pH 9 at 4 °C (as illustrated in Fig. 15(b)). The MUA-modified GNRs chosen, with an aspect ratio of 3.9, were further developed as a solution-phase-based label-free LSPR biosensor by functionalizing the GNRs with human IgG. A detection limit of as low as 0.4 nM, suitable for detecting anti-human IgG, was achieved by this sensor, indicating the MUA-modified GNRs prepared by the pH-mediated method proposed in this work could be used as an effective generic and sensitive, label-free biosensor platform.

## 5. GNR-based LSPR biosensors

As LSPR can be excited when light directly interacts with metallic nanoparticles, the design of LSPR sensors is more flexible than that of SPR sensors. Both the GNS-based and the GNR-based LSPR sensors can share the same sensor configuration, in which the sensors can be configured by either immobilizing gold nanoparticles on a transparent substrate such as a glass slide or just simply leaving functionalized nanoparticles suspended in the solution in a cuvette where the detection will take place after the addition of various analytes. In general, the configurations of GNR-based LSPR biosensors configurations can be classified into three categories: chip-based, optical fiber-based and solution-phase-based LSPR biosensors. Table 1 briefly summarizes some typical characteristics of these three configurations.

### 5.1. Chip-based LSPR sensor

The chip-based configuration is commonly used in the fabrication of LSPR sensors [15,31,81,97–99]. The chip-based LSPR sensor is normally fabricated by immobilizing GNRs on the surface of a flat transparent silica substrate, such as a glass slide and coverslip, without the need for a bulk prism as used in the SPR sensors. For GNRs synthesized by using the EBL technique or direct growth on the substrate, the sensor chip is simply obtained after the synthesis of the nanorods. For GNRs suspending in solution, such as for GNRs synthesized by using the seed-mediated growth method, there are two main methods that may be used for immobilizing GNRs. The first method uses electrostatic force [81] in which a clean substrate is first immersed into a polyelectrolyte solution to make the substrate surface have a charge that is opposite to the surface charge of GNRs. Then, this charged substrate is dipped into the GNR solution to coat the GNRs onto its surface via electrostatic force. However, such a coating of GNRs, prepared by this ‘electrostatic force method’ normally suffers from poor stability and poor uniformity. A second, more commonly used method is based on the SAM technique [15,97–100] in which a clean substrate is first modified by immersing the substrate in an alkylsilane solution, such as MPTMS, to form a thiol-terminated silane SAM on the substrate surface. Subsequently, the silanized substrate is incubated in a GNRs solution to form a monolayer of GNRs on the substrate surface via covalent bond. After the immobilization of the GNRs, the surface of the GNRs can be further functionalized with various receptors, following which the sensor chip is ready for a range of different applications. A UV–Vis spectrophotometer is then normally employed to measure the LSPR absorbance spectrum of GNRs based on the transmission mode.

Chilkoti and co-workers reported a chip-based LSPR biosensor using GNRs [15]. As illustrated in Fig. 16(a), the GNRs were coated on a mercaptosilane-modified glass substrate by a dip-coating method. In the refractive index sensitivity study carried out (illustrated in Fig. 16(b)), the sensor was immersed in different solvents

**Table 1**

Characteristics of GNR-based LSPR sensors with different configurations.

Sensor configuration	Characteristics	LSPR sensing method	Detector	Ref.
Chip-based	GNRs immobilized on a silica substrate	Based on refractive index change at GNR surface	Bulk UV-Vis spectrophotometer	[14]
Optical fiber-based	GNRs immobilized on a decladed optical fiber	Based on refractive index change at GNR surface	Mini spectrometer	[101]
Solution-phase-based	GNRs suspended in solution	Based on refractive index change at GNR surface; based on GNRs aggregation	Bulk UV-Vis spectrophotometer	[117,119]

with various refractive indexes, and the sensor was found to have a refractive index sensitivity of 252 nm/RIU, which is 5 times higher than a similar sensor based on spherical gold nanoparticles [101]. The surface of the GNRs was further functionalized with biotin and the streptavidin–biotin model was employed to evaluate the biosensing performance of the LSPR biosensor. By monitoring the LPB peak wavelength shift, the limit of detection of the sensor created was found to be 94 pM in PBS and 19 nM in serum. Hafner and coworkers reported a similar chip-based LSPR biosensor to monitor the biomolecular interactions in a flow cell [30]. Here antibodies were covalently bound to the surface of GNRs immobilized on the glass slide and binding of antigen was monitored by LSPR measurement. The results showed that the sensor has a LSPR sensitivity of 170 nm/RIU and a limit of detection of about 1 nM. As the mean aspect ratio of GNRs used in this work is relatively low (~3.3), the sensitivity and limit of detection would be expected to be further improved by employing GNRs with higher aspect ratio.

## 5.2. Optical fiber-based LSPR sensors

Optical fiber-based LSPR sensors have shown many advantages, including small sample volume requirement, simplified optical

design, remote sensing capability and resistance to electromagnetic interference [102,103] over alternative approaches. In 2003, Cheng and Chau first demonstrated the fabrication and application of an optical fiber-based LSPR sensor based on gold nanoparticles [104]. The sensor showed high sensitivity to the local refractive index change and the capability of working as a biochemical sensor. Since then, a large number of optical fiber-based LSPR sensors have been developed and reported for various applications [16,30,44,105–115]. The majority of these optical fiber-based LSPR sensors described in the literature were fabricated by immobilizing gold nanoparticles on the decladed fiber core of a multimode optical fiber. Fig. 17(a)–(c) illustrates a number of different designs such as transmission-based, reflection-based and U-shaped LSPR optical fiber sensors, respectively. LSPR is excited at the core–nanoparticle boundary when light is transmitted in the optical fiber. In addition, apart from multimode optical fiber based LSPR sensors, several LSPR sensors using LPGs and tapered single-mode fibers have also been reported [116–118]. However, most of these optical fiber-based LSPR sensors discussed in the literature were based on using spherical gold nanoparticles.

Recently, in work by the authors, the development of GNR-based LSPR optical fiber biosensors [102,103] was reported. As shown in Fig. 18(a) and (b), the sensor probe was prepared by covalently

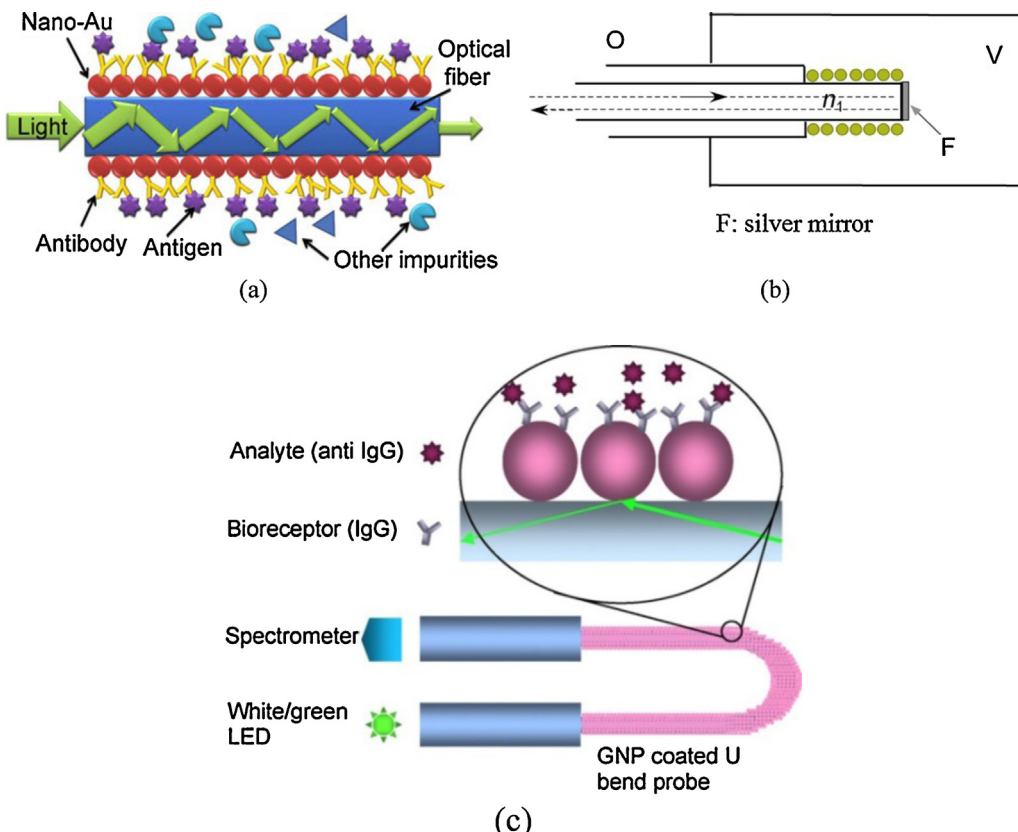


**Fig. 17.** Schematic illustration of optical fiber-based LSPR sensors with different configurations: (a) transmission-based LSPR optical fiber sensor. Reprinted with permission from Ref. [112]. (b) Reflection-based LSPR optical fiber sensor. Reprinted with permission from Ref. [105]. (c) U-shaped LSPR optical fiber sensor. Reprinted with permission from Ref. [44].

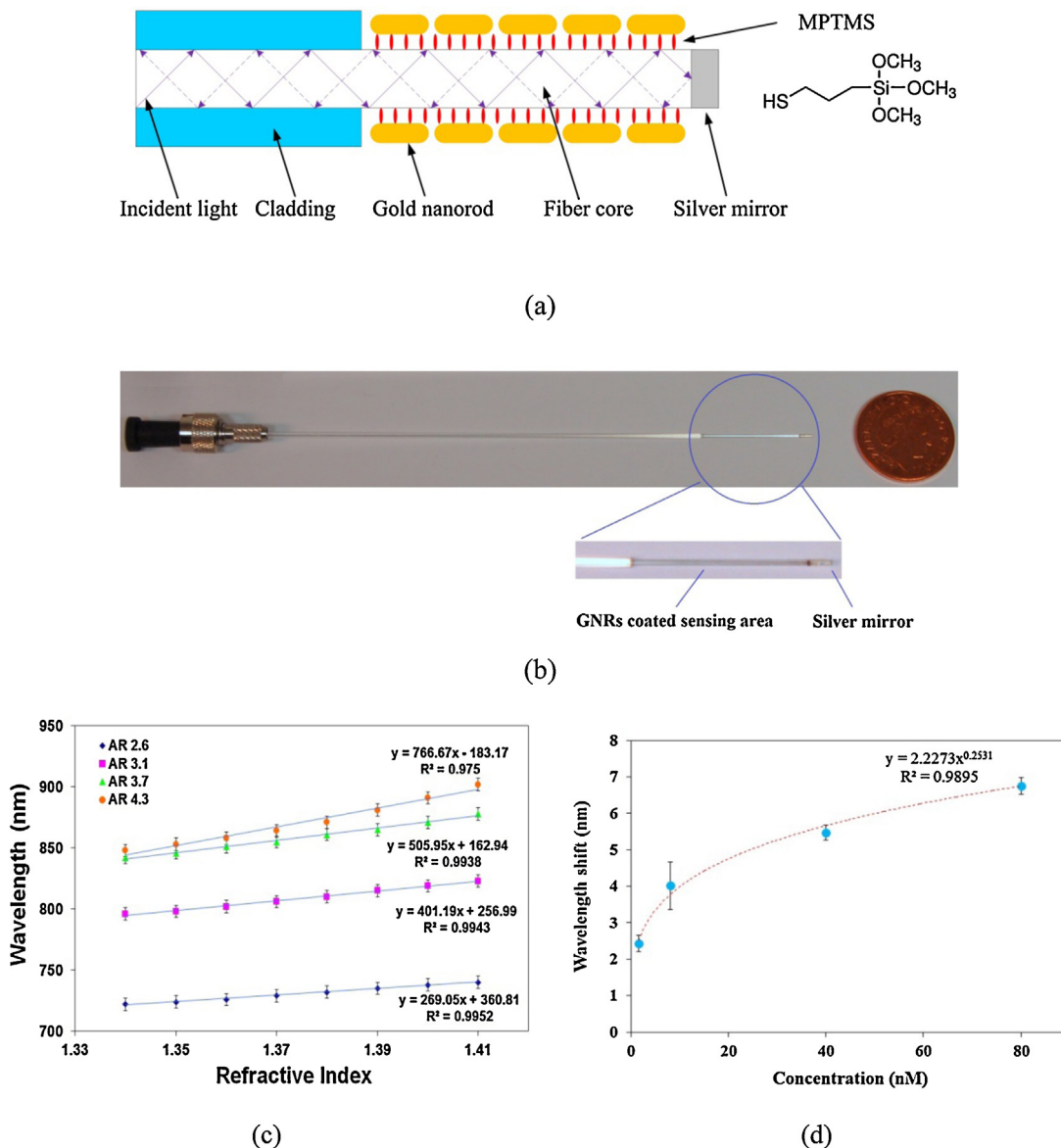


**Fig. 18.** (a) Schematic diagram of the structure of a GNR-coated LSPR optical fiber sensor, (b) photo of the as-prepared LSPR optical fiber sensor probe, (c) LPB peak wavelength shift of GNRs with four aspect ratios as a function of refractive index change, and (d) LPB peak wavelength shift of GNR-based LSPR biosensor as a function of concentration of anti-human IgG.

immobilizing GNRs which were synthesized using a seed-mediated growth method, on the decladched surface of a piece of multimode optical fiber. In order to operate the LSPR sensor as a reflective sensor, a silver mirror was also coated at the distal end of the sensor probe by using a simple dip coating method. In a test carried out to establish refractive index sensitivity, it was found that the LPB of GNRs is highly sensitive to the refractive index change close to the GNRs surface and the sensitivity of the LSPR optical fiber sensor increases with the increase of the aspect ratio of GNRs. The results showed that the GNR-based LSPR optical fiber sensors prepared in this work have both linear and high refractive index sensitivities. For sensors based on GNRs with aspect ratios of 2.6, 3.1, 3.7 and 4.3, their refractive index sensitivities were found to be 269, 401, 506 and 766 nm/RIU, respectively, in the refractive index range from 1.34 to 1.41 (as illustrated by Fig. 18(c)). In order to evaluate their performance in biosensing applications, a GNR-based LSPR optical fiber sensor with an aspect ratio of 4.1 was further functionalized with human IgG to detect the specific target—anti-human IgG, and a detection limit of 1.6 nM

was observed using a wavelength-based interrogation approach (as illustrated in Fig. 18(d)) [103].

### 5.3. Solution-phase-based LPSR sensor

Solution-phase-based LSPR sensors are those LSPR sensors with the gold nanoparticles suspended in solution rather than immobilized on a substrate [17,80,89,93,119–122]. This type of sensor allows the surface modification and functionalization of the gold nanoparticles as well as the detection of analytes to be carried out within the solution of gold nanoparticles. The fabrication of such a solution-phase-based LSPR sensor often involves gentle vortexing of the solution to mix fully the functional molecules and nanoparticles and multiple centrifugations to purify the functionalized nanoparticles. The analyte detection is normally conducted in a small container such as cuvette. Here a UV-Vis spectrophotometer used in the chip-based LSPR sensor is also applied for measuring the LSPR absorbance of the dispersed nanoparticles. For the solution-phase-based LSPR sensors using GNRs, there are two

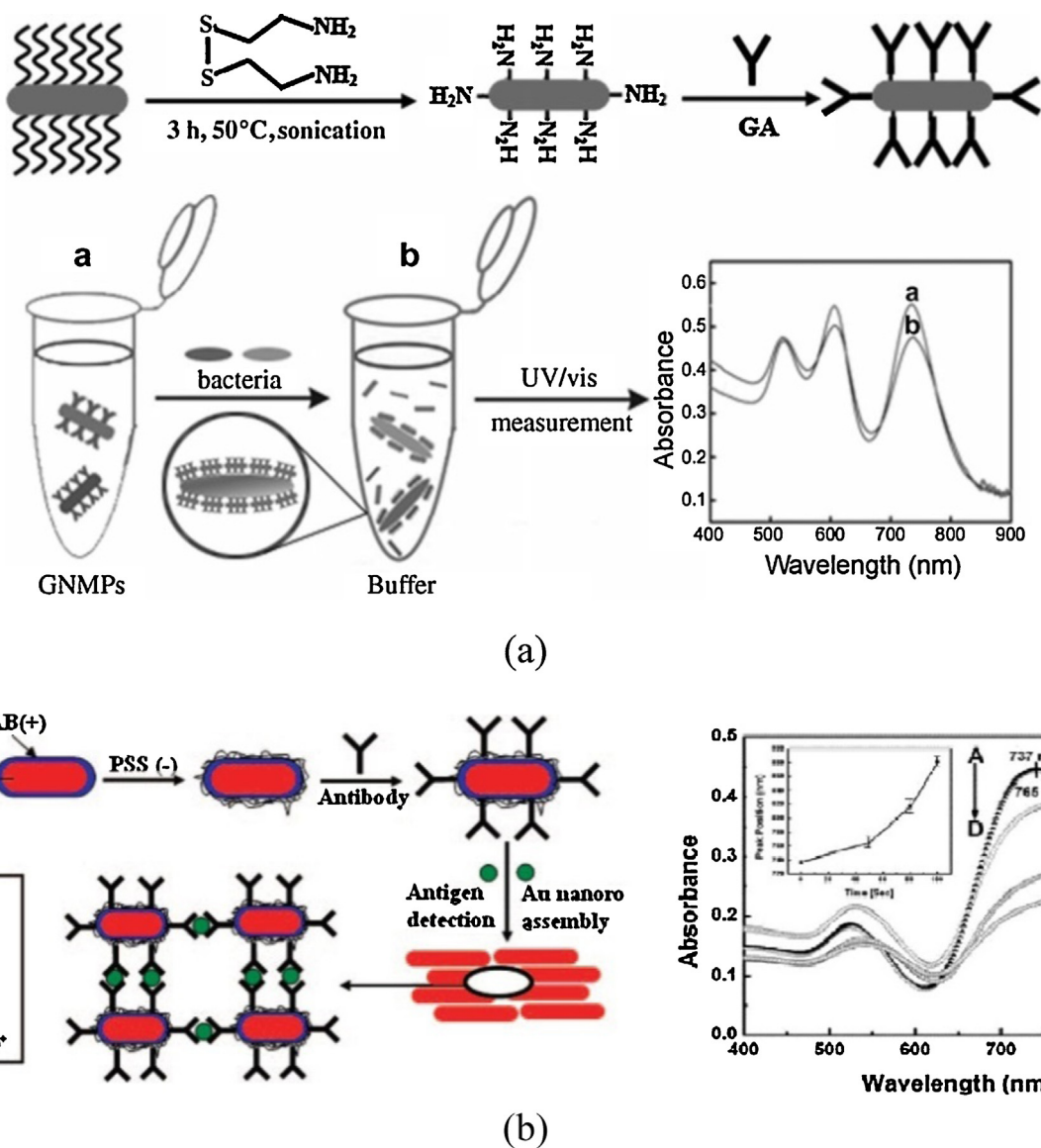


**Fig. 19.** (a) Schematic representation of the preparation of solution-phase-based LSPR sensor (top) and the detection of target molecules with many binding sites (bottom). Reprinted with permission from Ref. [120]. (b) Schematic representation of the detection of target molecules with few binding sites through the assembly of GNRs (left) and the corresponding absorption spectra changing over a period of time from A to D (right). Reprinted with permission from Ref. [121].

assays that are commonly employed for the detection of analytes: LSPR sensing based on refractive index change and LSPR sensing based on GNRs aggregation. Which assay should be applied is normally dependent on the number of the binding sites of the target molecule. If the target molecule has only one binding site, it will be captured by only one functionalized GNRs. The capture of the target molecule will result in a refractive index change at the GNR surface and a corresponding LSPR absorbance change, such as a red-shift of the longitudinal plasmon band of the GNRs based LSPR sensor. However, if there is more than one binding site on the surface for the target molecule, the same target molecule could be captured by GNRs as many times as the theoretical number of binding sites allows. If the target molecule has many binding sites, a number of capturing GNRs would be as demonstrated in Fig. 19(a); if the target molecule only has few binding sites, it normally would induce the assembly of the capturing GNRs as illustrated in Fig. 19(b). In either case, this will result in the eventual aggregation of the GNRs which will not only cause a color change of the GNR solution (that sometimes even can be identified with the naked eye) but also result in a large shift the LSPR absorption spectrum of the

nano-particles. However, the aggregation also substantially distorts the original LSPR spectrum of the dispersed nanoparticles, making the target molecules difficult to quantify accurately. Compared to the substrate-based LSPR sensors, the preparation of the solution-phase-based LSPR sensors is easier. However, in terms of their long-term stability, solution-phase-based LSPR sensors appear less stable than those that are substrate-based, due to the aggregation and deposition of GNRs over a longer period of time.

Wang et al. have demonstrated the detection of human IgG through the assembly of GNRs driven by antibody-antigen recognition [121]. The surface of CTAB-capped GNRs were first modified by using a negatively charged polyelectrolyte PSS to change the surface charge of the GNRs. Such negatively charged sites were then functionalized with anti-human IgG via electrostatic interaction. The aggregation of anti-human IgG functionalized GNRs occurred after the addition of human IgG, which resulted in a red-shift in the longitudinal plasmon band of GNRs and a broadening of the LSPR absorption spectrum. The peak position of longitudinal plasmon band of GNRs was monitored during the aggregation process and the LOD for human IgG was about 60 ng/mL. The

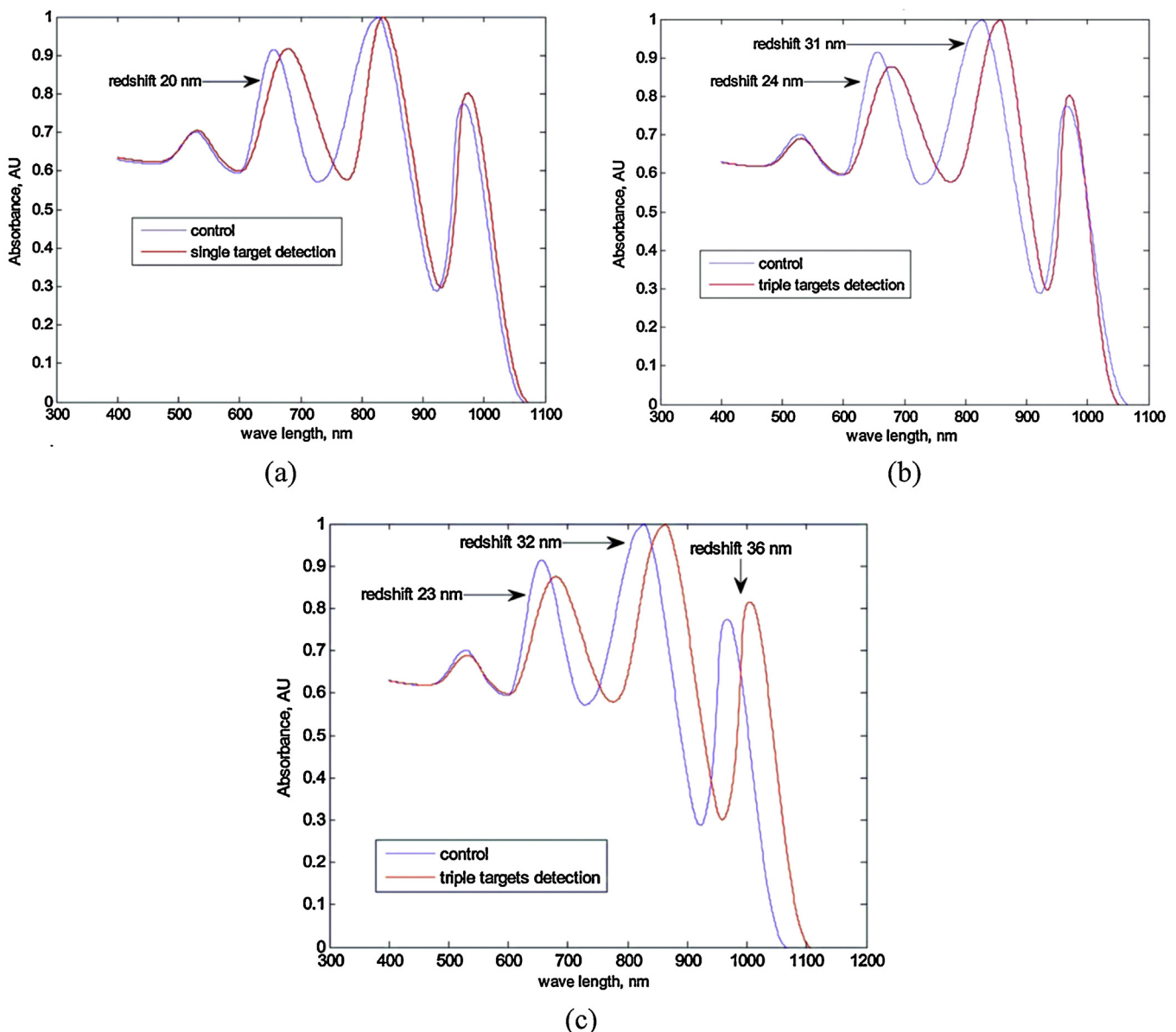


**Fig. 20.** Multiplexing detection of various targets using GNRs with different aspect ratios. (a) One target, (b) two targets and (c) three targets. Reprinted with permission from Ref. [119].

detection of a pervasive environmental toxin, microcystin-LR (MC-LR), using a LSPR biosensor based on the disassembly of GNRs had been reported by Wang et al. [123]. Two batches of GNRs were functionalized with MC-LR antibodies and MC-LR analogs respectively, having an affinity to MC-LR antibodies. The MC-LR antibodies and the MC-LR analogues conjugated GNRs were then mixed together, forming assemblies of GNRs and resulting in a decrease in the LSPR absorbance. The addition of MC-LR led to a competition for the antibody binding sites and a dissociation of assembled GNRs, thus gradually restoring the LSPR spectrum of the GNRs. By monitoring the peak absorbance change of the longitudinal plasmon band during the disassembling process, the LOD for MC-LR was found to be 0.6 ng/mL for the side-by-side assemblies of GNRs and 0.03 ng/mL for the end-to-end assemblies.

## 6. Advances in LSPR biosensing

Advances in two specific fields, multiplexing of biosensors and single-nanoparticle based LSPR biosensing are highlighted below.

### 6.1. Multiplexed biosensing

As metallic nanoparticles of different sizes and shapes possess different LSPR absorption bands, multiplexed LSPR biosensing can be realized by employing different metallic nanoparticles in the same assay. Using GNRs is often preferable to multiplexed sensing for the reason that the longitudinal plasmon band of GNRs can be conveniently tuned by controlling the aspect ratio of the GNRs. Yu and Irudayaraj have demonstrated a multiplexed biosensor for detecting multiple target molecules using GNRs of various aspect ratios [119]. In their work, GNRs with three different aspect ratios were functionalized with three different antibodies respectively, and mixed together to fabricate the solution-phased-based the multiplexed biosensor. Three different longitudinal plasmon bands corresponding to these three aspect ratios appearing in the LSPR absorption spectrum, as shown in Fig. 20. The addition of one target molecules resulted in a significant red-shift of one of the longitudinal plasmon bands due to target specific binding and a small red-shift in the other two longitudinal plasmon bands due to non-specific binding (Fig. 20(a)). This specific binding caused a red-shift

that is large enough to be distinguished from the two small red-shifts induced by non-specific binding. Likewise, the addition of either two targets and three targets has resulted in either two or three clear red-shifts in the longitudinal plasmon bands of the corresponding antibody-conjugated GNRs, respectively (Fig. 20(a) and (b)). Therefore, multiple targets can be detected at the same time by monitoring the wavelength shifts in the corresponding longitudinal plasmon bands. Later, they applied this multiplexed sensing technique to detect *Escherichia coli* and salmonella for food safety applications [120]. Based on the same principle, Huang et al. developed a chip-based multiplexed biosensor also using GNRs [31]. GNRs with various aspect ratios were immobilized on the separate glass slides, followed by functionalizing these GNRs with different antibodies respectively. These sensor chips were then assembled in a cuvette as the multiplexed sensor and the multiplexing sensing ability of the sensor was demonstrated by monitoring the peak absorbance change in each longitudinal plasmon band induced by the target specific binding.

## 6.2. Single-nanoparticle based LSPR biosensing

Most LSPR spectroscopy has been performed with ensembles of metallic nanoparticles; however, each individual nanoparticle in the ensembles could serve as an independent LSPR sensor [18,124]. Compared to the traditional nanoparticle array-based LSPR sensors, single-nanoparticle based LSPR sensors have shown advantages such as higher sensitivity, lower detection limit and very small sample volumes requirement [14,25]. Single-nanoparticle spectroscopy is normally performed by using a dark-field microscopy system. Fig. 21(a) shows an example of this in which a high-numerical aperture condenser brings white light to the sample and a low-numerical aperture microscope objective collects the scattered light at low angles. This scattered light is then directed to a spectrometer and detector, such as a charge-coupled device camera, yielding an LSPR spectrum of the sample [14]. The sample is prepared by immobilizing metallic nanoparticles on a transparent glass substrate. The label-free biosensing can be carried out by tracking the wavelength shift in the LSPR scattering spectrum of a single nanoparticle using the dark-field microscopy as demonstrated in Fig. 21(b). So far, apart from GNRs [124], metallic nanoparticles with other nanostructures such as silver nanoparticles [18], GNSs [125], GNRs, gold nanoholes [126] and gold nanorings [127] have been employed in developing

single-nanoparticle based LSPR biosensors. Despite the advantages of these single-nanoparticle based LSPR sensors, the low single-to-noise ratio still remains a big limitation for these sensors before they could be applied in practical applications in the future [128,129].

## 7. Conclusion and future outlook

In this review it can be seen that compared to other metallic nanoparticles, GNRs have shown both exceptional and highly desirable optical properties in LSPR-based biosensing applications, taking advantage of the high refractive index sensitivity and the potential for multiplexed sensing, all of which have attracted considerable attention from researchers focused on the development of GNR-based sensitive LSPR biosensors. Nevertheless, important challenges still remain in the practical implementation of such sensors and in the exploring of new research directions. First, compared to other synthesis methods, the seed-mediated growth approach has been widely applied for the synthesis of GNRs due to the ease of synthesis and high yield of GNRs. However, as it is known that many different parameters may affect the formation of GNRs, those GNRs produced through seed-mediated growth often suffer poor reproducibility, meaning that the aspect ratio and the LPB peak wavelength are often slightly different from batch to batch. Therefore, a cost-effective and robust approach for making GNRs with high reproducibility is still needed. Second, optical fiber-based LSPR biosensors have shown many advantages when compared to biosensors developed with other different configurations. However, most of those optical fiber LSPR biosensors previously reported were fabricated by using spherical nanoparticles, showing poor wavelength LSPR refractive index sensitivities. It is important to note that GNR-based optical fiber biosensors have shown higher sensitivity, as demonstrated in the work reported here. Combining the advantages of both GNRs and optical fiber sensors, increasingly sensitive and diverse GNR-based optical fiber LSPR biosensors are expected to be developed in near future. Finally, although the LSPR sensing technique has been applied in the development of label-free biosensors for detecting specific target molecules, the LSPR technique itself is non-specific sensing technique. This is because that the LSPR response is dependent only on the refractive index surrounding the nanoparticles, and the specificity is achieved through the molecular recognition involved, such as antigen-antibody recognition. All this means that LSPR is

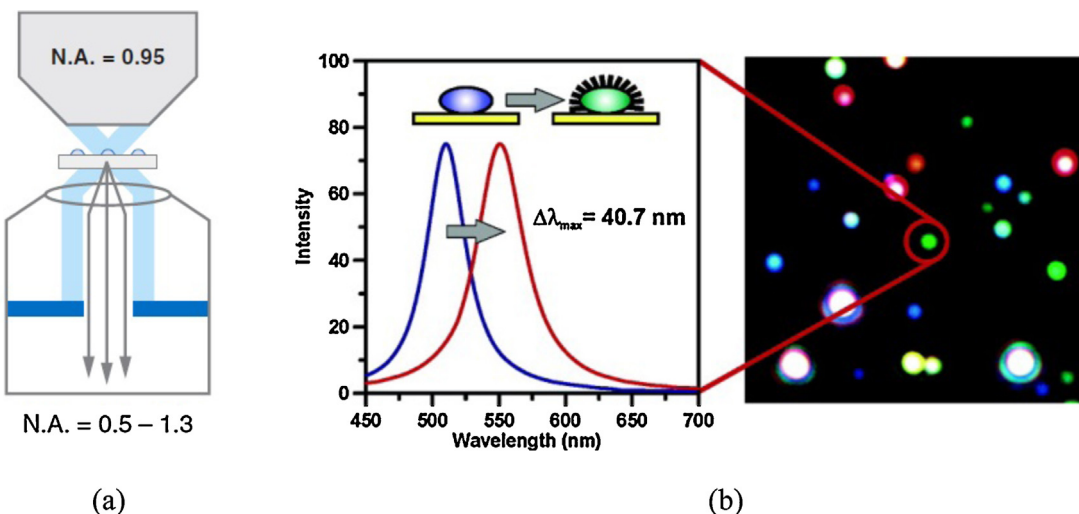


**Fig. 21.** (a) Schematic representation of a dark-field microscopy system for measuring single-nanoparticle scattering spectra. Reprinted with permission from Ref. [14]. (b) LSPR spectral shift induced by target molecules binding to a single silver nanoparticle (left), and the dark-field optical image of silver nanoparticles (right). Reprinted with permission from Ref. [18].

not a very suitable technique for the identification of unknown molecules. However, the combination of the LSPR technique with other identification techniques such as surface-enhanced Raman scattering (SERS) allows unknown molecules to be first characterized with LSPR and then identified with this identification technique and this has the potential to greatly expand the range of suitable applications of the LSPR technique in the future.

## Acknowledgements

The authors would like to thank the Engineering and Physical Sciences Research Council (EPSRC) in the UK for the funding support via various schemes. The support of the George Daniels Educational Trust is also greatly appreciated.

## References

- [1] S.M. Borisov, O.S. Wolfbeis, Optical biosensors, *Chemical Reviews* 108 (2008) 423–461.
- [2] D.R. Thevenot, K. Toth, R.A. Durst, G.S. Wilson, Electrochemical biosensors: recommended definitions and classification, *Biosensors & Bioelectronics* 16 (2001) 121–131.
- [3] J.C. Pickup, F. Hussain, N.D. Evans, O.J. Rolinski, D.J.S. Birch, Fluorescence-based glucose sensors, *Biosensors & Bioelectronics* 20 (2005) 2555–2565.
- [4] L.Y. Wang, R.X. Yan, Z.Y. Hao, L. Wang, J.H. Zeng, J. Bao, X. Wang, Q. Peng, Y.D. Li, Fluorescence resonant energy transfer biosensor based on upconversion-luminescent nanoparticles, *Angewandte Chemie International Edition* 44 (2005) 6054–6057.
- [5] P.J. Jiang, Z.J. Guo, Fluorescent detection of zinc in biological systems: recent development on the design of chemosensors and biosensors, *Coordination Chemistry Reviews* 248 (2004) 205–229.
- [6] J. Homola, Present and future of surface plasmon resonance biosensors, *Analytical and Bioanalytical Chemistry* 377 (2003) 528–539.
- [7] Q.M. Yu, S.F. Chen, A.D. Taylor, J. Homola, B. Hock, S.Y. Jiang, Detection of low-molecular-weight domoic acid using surface plasmon resonance sensor, *Sensors and Actuators B: Chemical* 107 (2005) 193–201.
- [8] J. Homola, Surface plasmon resonance sensors for detection of chemical and biological species, *Chemical Reviews* 108 (2008) 462–493.
- [9] J. Yakovleva, R. Davidsson, M. Bengtsson, T. Laurell, J. Emneus, Microfluidic enzyme immunoassays with immobilised protein A and G using chemiluminescence detection, *Biosensors & Bioelectronics* 19 (2003) 21–34.
- [10] J. Zhang, H.L. Qi, Y. Li, J. Yang, Q. Gao, C.X. Zhang, Electrogenerated chemiluminescence DNA biosensor based on hairpin DNA probe labeled with ruthenium complex, *Analytical Chemistry* 80 (2008) 2888–2894.
- [11] S. Scarano, M. Mascini, A.P.F. Turner, M. Minunni, Surface plasmon resonance imaging for affinity-based biosensors, *Biosensors & Bioelectronics* 25 (2010) 957–966.
- [12] J. Homola, S.S. Yee, G. Gauglitz, Surface plasmon resonance sensors: review, *Sensors and Actuators B: Chemical* 54 (1999) 3–15.
- [13] S. Eustis, M.A. El-Sayed, Why gold nanoparticles are more precious than pretty gold: noble metal surface plasmon resonance and its enhancement of the radiative and nonradiative properties of nanocrystals of different shapes, *Chemical Society Reviews* 35 (2006) 209–217.
- [14] K.A. Willets, R.P. Van Duyne, Localized surface plasmon resonance spectroscopy and sensing, *Annual Review of Physical Chemistry*, Annual Reviews, Palo Alto 58 (2007) 267–297.
- [15] S.M. Marinakos, S. Chen, A. Chilkoti, Plasmonic detection of a model analyte in serum by a gold nanorod sensor, *Analytical Chemistry* 79 (2007) 5278–5283.
- [16] K. Kajikawa, K. Mitsui, Optical fiber biosensor based on localized surface plasmon resonance in gold nanoparticles, in: M.S. Islam, A.K. Dutta (Eds.), *Nanosensing: Materials and Devices*, SPIE – Int. Soc. Optical Engineering, Bellingham, 2004, pp. 494–501.
- [17] M. Potara, A.M. Gabudean, S. Astilean, Solution-phase, dual LSPR-SERS plasmonic sensors of high sensitivity and stability based on chitosan-coated anisotropic silver nanoparticles, *Journal of Materials Chemistry* 21 (2011) 3625–3633.
- [18] A.D. McFarland, R.P. Van Duyne, Single silver nanoparticles as real-time optical sensors with zeptomole sensitivity, *Nano Letters* 3 (2003) 1057–1062.
- [19] A.V. Kabashin, P. Evans, S. Pastkovsky, W. Hendren, G.A. Wurtz, R. Atkinson, R. Pollard, V.A. Podolskiy, A.V. Zayats, Plasmonic nanorod metamaterials for biosensing, *Nature Materials* 8 (2009) 867–871.
- [20] X. Huang, S. Neretina, M.A. El-Sayed, Gold nanorods: from synthesis and properties to biological and biomedical applications, *Advanced Materials* 21 (2009) 4880–4910.
- [21] L. Vigderman, B.P. Khanal, E.R. Zubarev, Functional gold nanorods: synthesis, self-assembly, and sensing applications, *Advanced Materials* 24 (2012) 4811–4841.
- [22] Z.G. Xie, J. Tao, Y.H. Lu, K.Q. Lin, J. Yan, P. Wang, H. Ming, Polymer optical fiber SERS sensor with gold nanorods, *Optics Communication* 282 (2009) 439–442.
- [23] C.J. Murphy, A.M. Gole, S.E. Hunyadi, J.W. Stone, P.N. Sisco, A. Alkilany, B.E. Kinard, P. Hankins, Chemical sensing and imaging with metallic nanorods, *Chemical Communications* (2008) 544–557.
- [24] X. Huang, I.H. El-Sayed, W. Qian, M.A. El-Sayed, Cancer cell imaging and photothermal therapy in the near-infrared region by using gold nanorods, *Journal of the American Chemical Society* 128 (2006) 2115–2120.
- [25] J.N. Anker, W.P. Hall, O. Lyandres, N.C. Shah, J. Zhao, R.P. Van Duyne, Biosensing with plasmonic nanosensors, *Nature Materials* 7 (2008) 442–453.
- [26] V. Sharma, K. Park, M. Srinivasarao, Colloidal dispersion of gold nanorods: historical background, optical properties, seed-mediated synthesis, shape separation and self-assembly, *Materials Science & Engineering R – Reports* 65 (2009) 1–38.
- [27] E. Hutter, J.H. Fendler, Exploitation of localized surface plasmon resonance, *Advanced Materials* 16 (2004) 1685–1706.
- [28] S. Link, M.A. El-Sayed, Shape and size dependence of radiative, non-radiative and photothermal properties of gold nanocrystals, *International Reviews in Physical Chemistry* 19 (2000) 409–453.
- [29] S. Link, M.A. El-Sayed, Optical properties and ultrafast dynamics of metallic nanocrystals, *Annual Review of Physical Chemistry* 54 (2003) 331–366.
- [30] K.M. Mayer, S. Lee, H. Liao, B.C. Rostro, A. Fuentes, P.T. Scully, C.L. Nehl, J.H. Hafner, A label-free immunoassay based upon localized surface plasmon resonance of gold nanorods, *ACS Nano* 2 (2008) 687–692.
- [31] H. Huang, C.C. He, Y.L. Zeng, X.D. Xia, X.Y. Yu, P.G. Yi, Z. Chen, A novel label-free multi-throughput optical biosensor based on localized surface plasmon resonance, *Biosensors & Bioelectronics* 24 (2009) 2255–2259.
- [32] E. Petryayeva, U.J. Krull, Localized surface plasmon resonance: nanostructures, bioassays and biosensing – a review, *Analytica Chimica Acta* 706 (2011) 8–24.
- [33] K.M. Mayer, J.H. Hafner, Localized surface plasmon resonance sensors, *Chemical Reviews* 111 (2011) 3828–3857.
- [34] P.N. Njoki, I.I.S. Lim, D. Mott, H.Y. Park, B. Khan, S. Mishra, R. Sujakumar, J. Luo, C.J. Zhong, Size correlation of optical and spectroscopic properties for gold nanoparticles, *Journal of Physical Chemistry C* 111 (2007) 14664–14669.
- [35] R. Gans, Über die form ultramikroskopischer goldteilchen, *Annalen der Physik* 342 (1912) 881–900.
- [36] C.A. Foss, G.L. Hornyak, J.A. Stockert, C.R. Martin, Template-synthesized nanoscopic gold particles – optical-spectra and the effects of particle-size and shape, *Journal of Physical Chemistry* 98 (1994) 2963–2971.
- [37] S. Link, M.B. Mohamed, M.A. El-Sayed, Simulation of the optical absorption spectra of gold nanorods as a function of their aspect ratio and the effect of the medium dielectric constant, *Journal of Physical Chemistry B* 103 (1999) 3073–3077.
- [38] M. Hu, J. Chen, Z.-Y. Li, L. Au, G.V. Hartland, X. Li, M. Marquez, Y. Xia, Gold nanostructures: engineering their plasmonic properties for biomedical applications, *Chemical Society Reviews* 35 (2006) 1084–1094.
- [39] J. Perez-Juste, I. Pastoriza-Santos, L.M. Liz-Marzan, P. Mulvaney, Gold nanorods: synthesis, characterization and applications, *Coordination Chemistry Reviews* 249 (2005) 1870–1901.
- [40] L.S. Jung, C.T. Campbell, T.M. Chinowsky, M.N. Mar, S.S. Yee, Quantitative interpretation of the response of surface plasmon resonance sensors to adsorbed films, *Langmuir: The ACS Journal of Surfaces and Colloids* 14 (1998) 5636–5648.
- [41] A.J. Haes, R.P. Van Duyne, A nanoscale optical biosensor: sensitivity and selectivity of an approach based on the localized surface plasmon resonance spectroscopy of triangular silver nanoparticles, *Journal of the American Chemical Society* 124 (2002) 10596–10604.
- [42] M.C. Daniel, D. Astruc, Gold nanoparticles: assembly, supramolecular chemistry, quantum-size-related properties, and applications toward biology, catalysis, and nanotechnology, *Chemical Reviews* 104 (2004) 293–346.
- [43] J. Turkevich, P.C. Stevenson, J. Hillier, A study of the nucleation and growth processes in the synthesis of colloidal gold, *Discussions of the Faraday Society* 11 (1951) 55–75.
- [44] V.V.R. Sai, T. Kundu, S. Mukherji, Novel U-bent fiber optic probe for localized surface plasmon resonance based biosensor, *Biosensors & Bioelectronics* 24 (2009) 2804–2809.
- [45] N.R. Jana, L. Gearheart, C.J. Murphy, Seed-mediated growth approach for shape-controlled synthesis of spheroidal and rod-like gold nanoparticles using a surfactant template, *Advanced Materials* 13 (2001) 1389–1393.
- [46] N.R. Jana, L. Gearheart, C.J. Murphy, Wet chemical synthesis of high aspect ratio cylindrical gold nanorods, *Journal of Physical Chemistry B* 105 (2001) 4065–4067.
- [47] B. Nikoobakhsh, M.A. El-Sayed, Preparation and growth mechanism of gold nanorods (NRs) using seed-mediated growth method, *Chemistry of Materials* 15 (2003) 1957–1962.
- [48] X.C. Ye, L.H. Jin, H. Caglayan, J. Chen, G.Z. Xing, C. Zheng, D.N. Vicky, Y.J. Kang, N. Engheta, C.R. Kagan, C.B. Murray, Improved size-tunable synthesis of monodisperse gold nanorods through the use of aromatic additives, *ACS Nano* 6 (2012) 2804–2817.
- [49] C.J. Murphy, T.K. San, A.M. Gole, C.J. Orendorff, J.X. Gao, L. Gou, S.E. Hunyadi, T. Li, Anisotropic metal nanoparticles: synthesis, assembly, and optical applications, *Journal of Physical Chemistry B* 109 (2005) 13857–13870.
- [50] A. Gole, C.J. Murphy, Seed-mediated synthesis of gold nanorods: role of the size and nature of the seed, *Chemistry of Materials* 16 (2004) 3633–3640.
- [51] L.F. Gou, C.J. Murphy, Fine-tuning the shape of gold nanorods, *Chemistry of Materials* 17 (2005) 3668–3672.

- [52] X.C. Jiang, M.P. Pileni, Gold nanorods: influence of various parameters as seeds, solvent, surfactant on shape control, *Colloids and Surfaces A – Physicochemical and Engineering Aspects* 295 (2007) 228–232.
- [53] M.Z. Liu, P. Guyot-Sionnest, Synthesis and optical characterization of Au/Ag core/shell nanorods, *Journal of Physical Chemistry B* 108 (2004) 5882–5888.
- [54] D.K. Smith, B.A. Korgel, The importance of the CTAB surfactant on the colloidal seed-mediated synthesis of gold nanorods, *Langmuir: The ACS Journal of Surfaces and Colloids* 24 (2008) 644–649.
- [55] Y.Y. Yu, S.S. Chang, C.L. Lee, C.R.C. Wang, Gold nanorods: electrochemical synthesis and optical properties, *Journal of Physical Chemistry B* 101 (1997) 6661–6664.
- [56] S.S. Chang, C.W. Shih, C.D. Chen, W.C. Lai, C.R.C. Wang, The shape transition of gold nanorods, *Langmuir: The ACS Journal of Surfaces and Colloids* 15 (1999) 701–709.
- [57] R.M. Penner, C.R. Martin, Preparation and electrochemical characterization of ultramicroelectrode ensembles, *Analytical Chemistry* 59 (1987) 2625–2630.
- [58] C.R. Martin, Nanomaterials: a membrane-based synthetic approach, *Science* 266 (1994) 1961–1966.
- [59] C.R. Martin, Membrane-based synthesis of nanomaterials, *Chemistry of Materials* 8 (1996) 1739–1746.
- [60] B.M.I. van der Zande, M.R. Bohmer, L.G.J. Fokkink, C. Schonenberger, Colloidal dispersions of gold rods: synthesis and optical properties, *Langmuir: The ACS Journal of Surfaces and Colloids* 16 (2000) 451–458.
- [61] G.L. Hornyak, C.J. Patrissi, C.R. Martin, Fabrication, characterization, and optical properties of gold nanoparticle/porous alumina composites: the non-scattering Maxwell–Garnett limit, *Journal of Physical Chemistry B* 101 (1997) 1548–1555.
- [62] A. Boltasseva, Plasmonic components fabrication via nanoimprint, *Journal of Optics A – Pure and Applied Optics* 11 (2009) 114001.
- [63] L. Billot, M.L. de la Chapelle, A.S. Grimault, A. Vial, D. Barchiesi, J.L. Bijeon, P.M. Adam, P. Royer, Surface enhanced Raman scattering on gold nanowire arrays: evidence of strong multipolar surface plasmon resonance enhancement, *Chemical Physics Letters* 422 (2006) 303–307.
- [64] F. Kim, J.H. Song, P.D. Yang, Photochemical synthesis of gold nanorods, *Journal of the American Chemical Society* 124 (2002) 14316–14317.
- [65] O.R. Miranda, T.S. Ahmadi, Effects of intensity and energy of CWUV light on the growth of gold nanorods, *Journal of Physical Chemistry B* 109 (2005) 15724–15734.
- [66] N. Taub, O. Krichevski, G. Markovich, Growth of gold nanorods on surfaces, *Journal of Physical Chemistry B* 107 (2003) 11579–11582.
- [67] Y.J. Kim, G. Cho, J.H. Song, Synthesis of size and shape-selective Au nanocrystals via proton beam irradiation, *Nuclear Instruments & Methods in Physics Research Section B – Beam Interactions with Materials and Atoms* 246 (2006) 351–354.
- [68] G. Canizal, J.A. Ascencio, J. Gardea-Torresday, M.J. Yacaman, Multiple twinned gold nanorods grown by bio-reduction techniques, *Journal of Nanoparticle Research* 3 (2001) 475–481.
- [69] Y.J. Zhu, X.L. Hu, Microwave-polyol preparation of single-crystalline gold nanorods and nanowires, *Chemistry Letters* 32 (2003) 1140–1141.
- [70] J.M. Cao, X.J. Ma, M.B. Zheng, J.S. Liu, H.M. Ji, Solvothermal preparation of single-crystalline gold nanorods in novel nonaqueous microemulsions, *Chemistry Letters* 34 (2005) 730–731.
- [71] B. Nikoobakhht, M.A. El-Sayed, Evidence for bilayer assembly of cationic surfactants on the surface of gold nanorods, *Langmuir: The ACS Journal of Surfaces and Colloids* 17 (2001) 6368–6374.
- [72] C.J. Murphy, L.B. Thompson, D.J. Chernak, J.A. Yang, S.T. Sivapalan, S.P. Boullos, J. Huang, A.M. Alkilany, P.N.isco, Gold nanorod crystal growth: from seed-mediated synthesis to nanoscale sculpting, *Current Opinion in Colloid & Interface Science* 16 (2011) 128–134.
- [73] S.H. Brewer, W.R. Glomm, M.C. Johnson, M.K. Knag, S. Franzen, Probing BSA binding to citrate-coated gold nanoparticles and surfaces, *Langmuir: The ACS Journal of Surfaces and Colloids* 21 (2005) 9303–9307.
- [74] H. Li, L. Rothberg, Colorimetric detection of DNA sequences based on electrostatic interactions with unmodified gold nanoparticles, *Proceedings of the National Academy of Sciences of the United States of America* 101 (2004) 14036–14039.
- [75] X. Li, L. Jiang, Q. Zhan, J. Qian, S. He, Localized surface plasmon resonance (LSPR) of polyelectrolyte-functionalized gold-nanoparticles for bio-sensing, *Colloids and Surfaces A: Physicochemical and Engineering Aspects* 332 (2009) 172–179.
- [76] B.C. Rostro-Kohanloo, L.R. Bickford, C.M. Payne, E.S. Day, L.J.E. Anderson, M. Zhong, S. Lee, K.M. Mayer, T. Zal, L. Adam, C.P.N. Dinney, R.A. Drezek, J.L. West, J.H. Hafner, The stabilization and targeting of surfactant-synthesized gold nanorods, *Nanotechnology* 20 (2009) 434005.
- [77] A.P. Leonov, J. Zheng, J.D. Clogston, S.T. Stern, A.K. Patri, A. Wei, Detoxification of gold nanorods by treatment with polystyrenesulfonate, *ACS Nano* 2 (2008) 2481–2488.
- [78] E.E. Connor, J. Mwamuka, A. Gole, C.J. Murphy, M.D. Wyatt, Gold nanoparticles are taken up by human cells but do not cause acute cytotoxicity, *Small* 1 (2005) 325–327.
- [79] N.J. Durr, T. Larson, D.K. Smith, B.A. Korgel, K. Sokolov, A. Ben-Yakar, Two-photon luminescence imaging of cancer cells using molecularly targeted gold nanorods, *Nano Letters* 7 (2007) 941–945.
- [80] A. Gole, C.J. Murphy, Biotin-streptavidin-induced aggregation of gold nanorods: tuning rod-rod orientation, *Langmuir: The ACS Journal of Surfaces and Colloids* 21 (2005) 10756–10762.
- [81] A. Gole, C.J. Murphy, Polyelectrolyte-coated gold nanorods: synthesis, characterization and immobilization, *Chemistry of Materials* 17 (2005) 1325–1330.
- [82] C.S. Ah, S. Do Hong, D.J. Jang, Preparation of Au@Ag shell nanorods and characterization of their surface plasmon resonances, *Journal of Physical Chemistry B* 105 (2001) 7871–7873.
- [83] C.C. Huang, Z.S. Yang, H.T. Chang, Synthesis of dumbbell-shaped Au–Ag core-shell nanorods by seed-mediated growth under alkaline conditions, *Langmuir: The ACS Journal of Surfaces and Colloids* 20 (2004) 6089–6092.
- [84] L.M. Liz-Marzan, M. Giersig, P. Mulvaney, Synthesis of nanosized gold–silica core–shell particles, *Langmuir: The ACS Journal of Surfaces and Colloids* 12 (1996) 4329–4335.
- [85] S.O. Obare, N.R. Jana, C.J. Murphy, Preparation of polystyrene- and silica-coated gold nanorods and their use as templates for the synthesis of hollow nanotubes, *Nano Letters* 1 (2001) 601–603.
- [86] J. Perez-Juste, M.A. Correa-Duarte, L.M. Liz-Marzan, Silica gels with tailored, gold nanorod-driven optical functionalities, *Applied Surface Science* 226 (2004) 137–143.
- [87] I. Gorelikov, N. Matsuura, Single-step coating of mesoporous silica on cetyltrimethyl ammonium bromide-capped nanoparticles, *Nano Letters* 8 (2008) 369–373.
- [88] S. Pierrat, I. Zins, A. Breivogel, C. Sonnichsen, Self-assembly of small gold colloids with functionalized gold nanorods, *Nano Letters* 7 (2007) 259–263.
- [89] H.W. Liao, J.H. Hafner, Gold nanorod bioconjugates, *Chemistry of Materials* 17 (2005) 4636–4641.
- [90] T. Niidome, Y. Akiyama, K. Shimoda, T. Kawano, T. Mori, Y. Katayama, Y. Niidome, In vivo monitoring of intravenously injected gold nanorods using near-infrared light, *Small* 4 (2008) 1001–1007.
- [91] T. Niidome, M. Yamagata, Y. Okamoto, Y. Akiyama, H. Takahashi, T. Kawano, Y. Katayama, Y. Niidome, PEG-modified gold nanorods with a stealth character for in vivo applications, *Journal of Controlled Release* 114 (2006) 343–347.
- [92] D. Bartczak, A.G. Kanaras, Preparation of peptide-functionalized gold nanoparticles using one pot EDC/sulfo-NHS coupling, *Langmuir: The ACS Journal of Surfaces and Colloids* 27 (2011) 10119–10123.
- [93] C. Yu, L. Varghese, J. Irudayaraj, Surface modification of cetyltrimethylammonium bromide-capped gold nanorods to make molecular probes, *Langmuir: The ACS Journal of Surfaces and Colloids* 23 (2007) 9114–9119.
- [94] B. Thierry, J. Ng, T. Krieg, H.J. Griesser, A robust procedure for the functionalization of gold nanorods and noble metal nanoparticles, *Chemical Communications* (2009) 1724–1726.
- [95] Q. Dai, J. Coutts, J. Zou, Q. Huo, Surface modification of gold nanorods through a place exchange reaction inside an ionic exchange resin, *Chemical Communications* (2008) 2858–2860.
- [96] J. Cao, E.K. Galbraith, T. Sun, K.T.V. Grattan, Effective surface modification of gold nanorods for localized surface plasmon resonance-based biosensors, *Sensors and Actuators B: Chemical* 169 (2012) 360–367.
- [97] H.W. Huang, C.R. Tang, Y.L. Zeng, X.Y. Yu, B. Liao, X.D. Xia, P.G. Yi, P.K. Chu, Label-free optical biosensor based on localized surface plasmon resonance of immobilized gold nanorods, *Colloids and Surfaces B – Biointerfaces* 71 (2009) 96–101.
- [98] N. Nath, A. Chilkoti, Label-free biosensing by surface plasmon resonance of nanoparticles on glass: optimization of nanoparticle size, *Analytical Chemistry* 76 (2004) 5370–5378.
- [99] K. Fujiwara, H. Watarai, H. Itoh, E. Nakahama, N. Ogawa, Measurement of antibody binding to protein immobilized on gold nanoparticles by localized surface plasmon spectroscopy, *Analytical and Bioanalytical Chemistry* 386 (2006) 639–644.
- [100] K.C. Grabar, R.G. Freeman, M.B. Hommer, M.J. Natan, Preparation and characterization of au colloid monolayers, *Analytical Chemistry* 67 (1995) 735–743.
- [101] C.D. Chen, S.F. Cheng, L.K. Chau, C.R.C. Wang, Sensing capability of the localized surface plasmon resonance of gold nanorods, *Biosensors & Bioelectronics* 22 (2007) 926–932.
- [102] J. Cao, E.K. Galbraith, T. Sun, K.T.V. Grattan, Cross-comparison of surface plasmon resonance-based optical fiber sensors with different coating structures, *IEEE Sensors Journal* 12 (2012) 2355–2361.
- [103] J. Cao, M.H. Tu, T. Sun, K.T.V. Grattan, Wavelength-based localized surface plasmon resonance optical fiber biosensor, *Sensors and Actuators B: Chemical* 181 (2013) 611–619.
- [104] S.F. Cheng, L.K. Chau, Colloidal gold-modified optical fiber for chemical and biochemical sensing, *Analytical Chemistry* 75 (2003) 16–21.
- [105] T.J. Lin, C.T. Lou, Reflection-based localized surface plasmon resonance fiber-optic probe for chemical and biochemical sensing at high-pressure conditions, *Journal of Supercritical Fluids* 41 (2007) 317–325.
- [106] T.J. Lin, M.F. Chung, Detection of cadmium by a fiber-optic biosensor based on localized surface plasmon resonance, *Biosensors & Bioelectronics* 24 (2009) 1213–1218.
- [107] W.H. Ni, H.J. Chen, X.S. Kou, M.H. Yeung, J.F. Wang, Optical fiber-excited surface plasmon resonance spectroscopy of single and ensemble gold nanorods, *Journal of Physical Chemistry C* 112 (2008) 8105–8109.
- [108] K. Mitsui, Y. Handa, K. Kajikawa, Optical fiber affinity biosensor based on localized surface plasmon resonance, *Applied Physics Letters* 85 (2004) 4231–4233.
- [109] S.K. Srivastava, V. Arora, S. Sapra, B.D. Gupta, Localized surface plasmon resonance-based fiber optic U-shaped biosensor for the detection of blood glucose, *Plasmonics* 7 (2012) 261–268.

- [110] Y.B. Lin, Y. Zou, R.G. Lindquist, A reflection-based localized surface plasmon resonance fiber-optic probe for biochemical sensing, *Biomedical Optics Express* 2 (2011) 478–484.
- [111] R. Dutta, R. Bharadwaj, S. Mukherji, T. Kundu, Study of localized surface-plasmon-resonance-based optical fiber sensor, *Applied Optics* 50 (2011) E138–E144.
- [112] C.H. Chen, T.C. Tsao, W.Y. Li, W.C. Shen, C.W. Cheng, J.L. Tang, C.P. Jen, L.K. Chau, W.T. Wu, Novel U-shape gold nanoparticles-modified optical fiber for localized plasmon resonance chemical sensing, *Microsystem Technologies* 16 (2010) 1207–1214.
- [113] T.J. Lin, M.F. Chung, Using monoclonal antibody to determine lead ions with a localized surface plasmon resonance fiber-optic biosensor, *Sensors* 8 (2008) 582–593.
- [114] B.Y. Hsieh, Y.F. Chang, M.Y. Ng, W.C. Liu, C.H. Lin, H.T. Wu, C. Chou, Localized surface plasmon coupled fluorescence fiber-optic biosensor with gold nanoparticles, *Analytical Chemistry* 79 (2007) 3487–3493.
- [115] L.K. Chau, Y.F. Lin, S.F. Cheng, T.J. Lin, Fiber-optic chemical and biochemical probes based on localized surface plasmon resonance, *Sensors and Actuators B: Chemical* 113 (2006) 100–105.
- [116] J.L. Tang, S.F. Cheng, W.T. Hsu, T.Y. Chiang, L.K. Chau, Fiber-optic biochemical sensing with a colloidal gold-modified long period fiber grating, *Sensors and Actuators B: Chemical* 119 (2006) 105–109.
- [117] J.L. Tang, J.N. Wang, Chemical sensing sensitivity of long-period grating sensor enhanced by colloidal gold nanoparticles, *Sensors* 8 (2008) 171–184.
- [118] H.Y. Lin, C.H. Huang, G.L. Cheng, N.K. Chen, H.C. Chui, Tapered optical fiber sensor based on localized surface plasmon resonance, *Optics Express* 20 (2012) 21693–21701.
- [119] C.Yu, J. Irudayaraj, Multiplex biosensor using gold nanorods, *Analytical Chemistry* 79 (2007) 572–579.
- [120] C. Wang, J. Irudayaraj, Gold nanorod probes for the detection of multiple pathogens, *Small* 4 (2008) 2204–2208.
- [121] C.G. Wang, Y. Chen, T.T. Wang, Z.F. Ma, Z.M. Su, Biorecognition-driven self-assembly of gold nanorods: a rapid and sensitive approach toward antibody sensing, *Chemistry of Materials* 19 (2007) 5809–5811.
- [122] P.K. Sudeep, S.T.S. Joseph, K.G. Thomas, Selective detection of cysteine and glutathione using gold nanorods, *Journal of the American Chemical Society* 127 (2005) 6516–6517.
- [123] L.B. Wang, Y.Y. Zhu, L.G. Xu, W. Chen, H. Kuang, L.Q. Liu, A. Agarwal, C.L. Xu, N.A. Kotov, Side-by-side and end-to-end gold nanorod assemblies for environmental toxin sensing, *Angewandte Chemie International Edition* 49 (2010) 5472–5475.
- [124] G.J. Nusz, S.M. Marinakos, A.C. Curry, A. Dahlin, F. Hook, A. Wax, A. Chilkoti, Label-free plasmonic detection of biomolecular binding by a single gold nanorod, *Analytical Chemistry* 80 (2008) 984–989.
- [125] G. Raschke, S. Kowarik, T. Franzl, C. Sonnichsen, T.A. Klar, J. Feldmann, A. Nichtl, K. Kurzinger, Biomolecular recognition based on single gold nanoparticle light scattering, *Nano Letters* 3 (2003) 935–938.
- [126] T. Rindzevicius, Y. Alaverdyan, A. Dahlin, F. Hook, D.S. Sutherland, M. Kall, Plasmonic sensing characteristics of single nanometric holes, *Nano Letters* 5 (2005) 2335–2339.
- [127] E.M. Larsson, J. Alegret, M. Kall, D.S. Sutherland, Sensing characteristics of NIR localized surface plasmon resonances in gold nanorings for application as ultrasensitive biosensors, *Nano Letters* 7 (2007) 1256–1263.
- [128] B. Sepulveda, P.C. Angelome, L.M. Lechuga, L.M. Liz-Marzan, LSPR-based nanobiosensors, *Nano Today* 4 (2009) 244–251.
- [129] A.B. Dahlin, S. Chen, M.P. Jonsson, L. Gunnarsson, M. Kall, F. Hook, High-resolution microspectroscopy of plasmonic nanostructures for miniaturized biosensing, *Analytical Chemistry* 81 (2009) 6572–6580.

## Biographies

**Jie Cao** received the B.E. degree in Electrical and Electronic Engineering from Harbin University of Science and Technology, Harbin, China, in 2004 and the M.E. degree in Mechatronic Engineering from Harbin Institute of Technology, Harbin, China, in 2007. He recently received the Ph.D. degree in Measurement and Instrumentation from City University London, London, UK. His research is focused on the design and fabrication of the SPR and LSPR based optical fiber sensors, and their biosensing applications.

**Tong Sun** received the B.E., M.E., and Dr. Eng. degrees in mechanical engineering from the Department of Precision Instrumentation, Harbin Institute of Technology, Harbin, China, in 1990, 1993, and 1998, respectively, and the Ph.D. degree in applied physics from the City University London, London, UK, in 1999. She is a Professor at the City University London, a member of the Institute of Physics and of the Institution of Engineering and Technology, and a Chartered Physicist and a Chartered Engineer in the UK.

**Kenneth T.V. Grattan** received the B.Sc. degree in physics from the Queen's University Belfast, Belfast, UK, in 1974, the Ph.D. degree in laser physics in 1979, and the D.Sc. degree from the City University London, London, UK, in 1992. He is a Professor at City University London, and the Dean of the City Graduate School, having formerly been Dean of the Schools of Engineering and Mathematical and Informatics. Prof. Grattan is a member of the Editorial Board of several major journals. He was awarded the Calendar Medal of the Institute of Measurement and Control in 1992, and the Honeywell Prize for work published in the Institute's journal as well as the Hartley Medal in 2012. He is a Fellow of the Royal Academy of Engineering, the UK National Academy for the field.